14. Origin of Diastereoselectivity in the Thermal [4+2] Cycloadditions of Dienophiles Derived from *Oppolzer*'s Sultams: Steric *vs.* Stereoelectronic Influences[1])

by **Christian Chapuis***, **Jean-Yves de Saint Laumer** and **Maurus Marty**[2])

Firmenich SA, Corporate Research Division, P.O.B. 239, CH-1211 Geneva 8

Dedicated to the memory of Professor *Wolfgang von Oppolzer*

(30.VIII.96)

Comparative semi-empirical PM3 and *ab initio* STO 3-21G calculations on bornanesultam-derived dienophiles containing the structural moiety SO_2–N–C(O)–X(α) = Y(β) suggest that, among the conformers of low energy, the thermodynamically less stable SO_2/C(O)-*syn*,C(O)/X=Y-s-*cis* conformation is also reactive in terms of LUMO level and atomic coefficients. Furthermore, the X(α), Y(β) LUMO atomic coefficients are nonequivalent with respect to both X(α)-*re* and X(α)-*si* faces, and thus have, depending on the conformation, a matching or mismatching stereoelectronic influence with the co-operative steric effect. This dissymmetry is believed to result from the generalized anomeric effect of the N lone pair, itself anomerically stabilized and directed, in the absence of crucial steric interactions, by the pseudo-axial *anti*-periplanar S=O bond. Five *N*-acyl-substituted bornanesultams are discussed ((–)-**1a**: *N*-acryloyl, X=CH, Y=CH_2; (–)-**1b**: *N*-crotonoyl, X=CH, Y=CHMe; (–)-**1c**: *N*,*N*′-fumaroyl, X=CH, Y=CH(C(O)-bornanesultam); **2a**: *N*-glyoxyloyl, X=CH, Y=O; **2b**: *N*-acylnitroso, X=N, Y=O). In this context, differences with toluenesultams **3** are pointed out. A previous report on *N*-(acylnitroso)-bornanesultam **2b** is revisited, and the diastereoselectivity observed is shown to result from thermodynamic control.

Introduction. – Current explanations of the diastereoselection observed in non-catalysed [4+2] cycloadditions[3]) of *N*-acyl dienophiles with the partial structure SO_2–N–C(O)–X(α)=Y(β) derived from *Oppolzer*'s bornane-10, 2- or toluenesultams[4]) are all based on the assumption that the reactive conformer is the thermodynamically most stable [2]. This conformer is assumed to have a SO_2/C(O)-*anti*,C(O)/C=C-s-*cis* conformation (X = Y = C), according to X-ray structure analyses in the crystalline state (see [3] for (–)-**1b**) and ^{1}H-NMR analyses in the presence of [Eu(fod)$_3$] [4] [5a]. A SO_2/C(O)-*anti*,C(O)/C=C-s-*trans* conformation has been also suggested by X-ray structure elucidation of C(α)-substituted dienophiles (see [5a] for (–)-**1e**), and ^{1}H-NOE measurements associated with MMX calculations [6]. Finally, a SO_2/C(O)-*syn*,C(O)/N=O-s-*cis* conformation has been postulated for **2b** according to *ab initio* LCAO-SCF-MO calculations [7]. The discrimination between the two faces of the reactive π-system has been explained by a steric approach, initially directed by the bornane Me(8) group [8], and,

[1]) Presented in part at the IXth Eur. Symp. Org. Chem., 18–23 June 1995, Warsaw, Poland.

[2]) Post-doctoral fellow at *Firmenich SA* from November 1995 to April 1996. Present address: University of Cambridge, Chemical Laboratory, Lensfield Road, Cambridge, England, CB2 1EW, UK.

[3]) For a recent review on asymmetric intermolecular homo- and hetero-*Diels-Alder* reactions, see [1].

[4]) Derived from saccharine (= 1,2-benzoisothiazol-3(2*H*)-one, 1,1-dioxide).

more recently, rationalized by *Kim* and *Curran* who visualize the system as a disguised C_2-symmetrical 2,5-disubstituted pyrrolidine [9], thus recognising the steric influence of the SO_2 moiety [10].

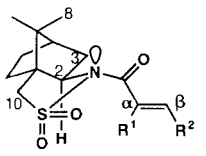

(–)-**1a** R^1 = H, R^2 = H
(–)-**1b** R^1 = H, R^2 = Me
(–)-**1c** R^1 = H, R^2 = C(O)-(2*R*)-bornanesultam
(–)-**1d** R^1 = Me, R^2 = H
(–)-**1e** R^1 = Me, R^2 = Me

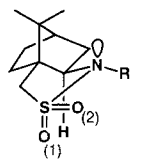

2a R = C(O)-CHO
2b R = C(O)-NO
(–)-**2c** R = H
2d R = C(O)Cl
(–)-**2e** R = C(O)-NHOH
(–)-**2f** R = C(O)-C(O)Me

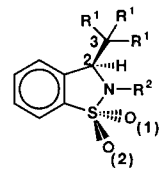

(–)-**3a** R^1 = H, R^2 = C(O)CH=CH_2
(–)-**3b** R^1 = Me, R^2 = C(O)CH=CH_2
(+)-**3c** R^1 = H, R^2 = H
(+)-**3d** R^1 = Me, R^2 = H
(–)-**3e** R^1 = H, R^2 = C(O)CH=CHMe

Both *Oppolzer* and *Curran* also invoked the possible electronic influence of the N lone pair [5] [10], which has been later discounted [9] in view of the poor correlation of the diastereoselectivity and the electronic nature of the attacking reagent[5]), as well as the fact that the reactive sites are not directly connected to the N-atom[6]). Blinkered by the initial steric approach to the thermodynamically most stable conformer, as well as by the supposed similar reactivities of both *syn* and *anti* conformers [9], our initial doubts[7]) [14] were strengthened after the reported cycloadditions of *N*-methacryloyl-bornanesultams (–)-**1d** [15]. With respect to the initial rationalization [5a], the stereochemistry observed cannot be based on the topicity of its X-ray structure analysis [16][8]). Bearing in mind the *Curtin-Hammett* principle [18], we turned our attention to finding the most reactive rather than the most stable species, under the assumption that a more reactive minor conformer would be able to drive the reaction by influencing the thermodynamic equilibrium.

Results and Discussion. – Using perturbation theory, *Klopman* [19] and *Salem* [20] have derived an appropriate expression to estimate the chemical reactivity which may be summarized as follows:

$$\Delta E = \underbrace{-\sum_{ab}(q_a + q_b)\beta_{ab}S_{ab}}_{\textit{first term}} + \underbrace{\sum_{k<l}\frac{Q_kQ_l}{\epsilon R_{kl}}}_{\textit{second term}} + \underbrace{\sum_{r}^{\text{occ.}}\sum_{s}^{\text{unocc.}} - \sum_{s}^{\text{occ.}}\sum_{r}^{\text{unocc.}}\frac{2(\sum_{ab}c_{ra}c_{sb}\beta_{ab})^2}{E_r - E_s}}_{\textit{third term}}$$

[5]) See page 311 and reference 48a in [9]. For an example of dependence on the nature of the attacking reagent on stereoselectivity, rationalized by an open transition state, see [11] [12].

[6]) For the first hypothesis of a π-face-directing effect of the N lone pair on electrophilic attack of enamines and N,O-ketene acetals, see [13].

[7]) First raised by a question of Prof. *Kündig* during the Ph.D. presentation of *C. C.* (December 1984), relating to the non-generality of the Me(8) directing effect when comparing the catalysed with the noncatalysed process. This problem could be later resolved by consideration of *Curran*'s postulate.

[8]) For a similar *anti*-s-*trans* X-ray structure of *N*-tigloyl-bornanesultam, see [5a]; for a postulated chelated *syn*-s-*cis* transition state, see [17].

When the problem is treated in solution, an additional term may be added which represents the energy of partial desolvation of the reactants as they form the adduct[9]). The first term, involving the electron densities (q) in the atomic orbitals a and b, as well as the resonance (β) and overlap (S) integrals, is the first-order closed-shell repulsion term and is usually very similar for each of two possible pathways. Thus, if there are two possible orientations for a cycloaddition, the first term, to a first approximation and in absence of sterical clash, remains constant [22]. The second term, obviously important when ions or polar molecules react together, is the *Coulomb* repulsion or attraction and includes the total charge (Q) on each atom k and l, separated, with the local dielectric constant (ε), by the distance R. The third term is the second-order perturbation term calculated from the energies of molecular orbitals r and s, and from the coefficients of atomic orbitals a and b in molecular orbitals r and s, respectively, which are located on the different molecules.

The reactivity, as described by the third term, increases for large atomic coefficients and for small differences between the frontier orbitals. Since the numerator is a square function, a small difference in atomic coefficients may result in a non-negligible impact on the reactivity. There are two extreme cases. One is when the atomic coefficients tend to zero, thus minimizing the third term to the advantage of the electrostatic term, and the second is when the two MO energies are almost equal. In this latter case, the interaction is better described in charge-transfer terms. Specifically, for the [4 + 2] cycloadditions studied here, one should consider the lowest LUMO energy associated with the largest atomic coefficients of the different dienophile conformers, in relation to the constant values adopted for the atomic coefficients and the HOMO of the diene[10]). Unfortunately, it is not obvious to determine experimentally the conformation of the reactive species [5a] [14], especially in the case of dienophiles (−)-**1** and **2**, since both minor and major conformers can give rise to the same stereochemical result [9]. To resolve this problem, we calculated the energies of the transition states[11]), choosing semi-empirical calculations due to the size of the molecules[12]). We restrained ourselves to the uncatalyzed cycloadditions reported in the literature, in view of the difficulty in obtaining fully optimized parameters for the metals chelated to unusual moieties such as N–SO_2 and N–C(O) as well as to avoid discussion of the relative reactivities of complexes, whose geometries can be linear [24], bent in the chelating plane [25], or bent out of the chelating plane [26].

The first example reported was the addition of cyclopentadiene to *N*-acryloyl-bornanesultam (−)-**1a** at 21° which gives, in an *endo* cycloaddition (89%), preferential C(α)-*re* face attack with 66% d.e. [4] [27]. Calculations at the PM3 level of theory are summarized in *Table 1*[13]) and confirm that the most stable planar conformer of (−)-**1a** is

---

[9]) For a study of MO reactivity base on photoelectron spectroscopic (PES) measurements, see [21].

[10]) PM3 Calculations for cyclopentadiene, 1-methoxybuta-1,3-diene, and acetonitrile oxide give the following values for the HOMO [eV], LUMO [eV] and ΔH_{form} [kcal/mol]: −9.23, 0.32, and 31.75, −8.85, 0.35, and −8.78, and −10.30, 1.22, and 21.04, respectively.

[11]) Comparing different conformers of the dienophile with the same diene under identical reaction conditions, the difference of entropy may be considered as very small and, thus, $\Delta\Delta H^{\neq}_{form}$ should reflect $\Delta\Delta G^{\neq}$ in the transition states.

[12]) For pericyclic reaction transitions states and semi-empirical studies of asymmetric *Diels-Alder* reactions, see [23].

[13]) For all PM3/AM1 conformational calculations of the dienophiles, reported in *Tables 1–7*, as well as their directly linked detailed *Tables 9–13* and *15–17*, the torsional angles were constrained to 0 or 180° with a force of 0.05 mdyn/Å^2 for S–N–C=O and 0.2 mdyn/Å^2 for O=C–X=Y torsional angles. Ground and transition states as well as STO3-21G conformational analyses were performed without constraints.

anti-s-*cis*, as earlier stated by *Oppolzer* and coworkers [3][14]). The first *trans* conformer is 3.91 kcal/mol higher in energy, representing at room temperature less than 0.05% of all possible conformers[15]). Based on the LUMO level, the *anti*-s-*cis* conformer apparently seems to be the most reactive species, although a careful examination shows that, among those of low conformational energy, the *syn*-s-*cis* conformer has larger C(α) and C(β) atomic coefficients. In addition, all conformers show more important atomic coefficients on the face opposite to the N lone pair. This stereoelectronic influence is mismatching the steric effect in the *anti*-s-*cis* conformation, whilst being additive in the *syn*-s-*cis* disposition. Thus, if for the *endo* transition state, the C(α)-*re*-face attack occurs on the *anti*-s-*cis* conformer as earlier proposed [3] [5]; attack on the same face with the *syn*-s-*cis* conformation, leading to the same cycloadduct, is energetically favourable compared to the C(α)-*si*-face attack, which leads to the minor diastereoisomer[16]) (see *Table 1*).

Table 1. *PM3 Values Calculated for the Cycloaddition of (–)-* **1a** *to Cyclopentadiene* (see *Fig. 1*)

Conformer	ΔH_{form} [kcal/mol]	LUMO [eV]	C(α)-*re* at. coef.	C(β)-*re* at. coef.
syn-s-*trans*	–88.03	–0.516	–0.065	0.075
anti-s-*trans*	–86.75	–0.738	*0.055*	*–0.030*
syn-s-*cis*	*–90.34*	–0.449	*0.075*	*–0.056*
anti-s-*cis*	*–91.94*	–0.604	–0.030	0.030
Conformer	**C(α)-*si* at. coef.**	**C(β)-*si* at. coef.**	**$\Delta H^{\neq}$ (C(α)-*re*) [kcal/mol]**	**$\Delta H^{\neq}$ (C(α)-*si*) [kcal/mol]**
syn-s-*trans*	*0.095*	*–0.080*	–20.56	–22.41
anti-s-*trans*	–0.032	0.030	–19.76	–24.87
syn-s-*cis*	–0.045	0.040	*–26.20*	–25.40
anti-s-*cis*	*0.050*	*–0.045*	*–28.18*	*–26.17*

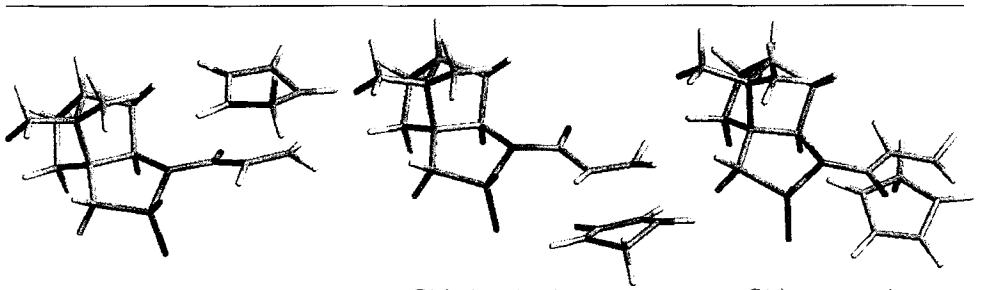

C(α)-*re anti*-s-*cis* C(α)-*si anti*-s-*cis* C(α)-*re syn*-s-*cis*

Fig. 1. *The three transition states participating to the stereochemical outcome of the cyclopentadiene addition to* (–)-**1a**

[14]) The ground-state energies expressed in kcal/mol for (–)-**1a**,**b**,**c**, **2a**,**b**, and (–)-**3a**,**b** are the following: –92.4, –103.14, –198.5, –138.6, –90.7, –61.2, and –72.2, respectively, corresponding to an *anti*-s-*cis* conformation with, in absolute value, a O=C–X=Y dihedral angle $\geq 3°$. The enthalpy of each *Diels-Alder* reaction at infinite separation of the reactants is obtained by summing with the ΔH_{form} of the dienes (see *Footnote 10*).

[15]) Throughout this work, we shall concentrate our discussion to the conformers which do not exceed the minimum energy by more than 3.5 kcal/mol. For the transition states, we chose 2.5 kcal/mol, since this corresponds to the limit of detection of NMR spectroscopy usually used for the analytical data reported.

[16]) C(α)-*re* and C(α)-*si* transition states derived from s-*cis* and s-*trans* orthogonal conformations (S–N–C=O = + or –90° [28]) were found to be much higher in energy (minimum *ca.* 5 kcal/mol). For each conformer, the C(α)-*re* and C(α)-*si* transition state approaches were recalculated for different positive and negative O=C–X=Y 'twisting angles', as earlier postulated as the origin for the observed diastereoselectivity [29], but were found to have no influence on the final results.

In the same publications [4] [27], thermal cycloaddition of *N*-crotonoyl-bornanesultam (−)-**1b** to cyclopentadiene is also reported to afford a lower π-facial selectivity (52% d.e.) in favour of the C(α)-*re* face for the *endo* cycloaddition (79%). This result is consistent with calculations; indeed, this face is more accessible for the *anti*-s-*cis* conformer (see *Table 2*). Furthermore, the minor *syn*-s-*cis* conformer of (−)-**1b** also reacts preferably on the C(α)-*re* face but, compared to the *N*-acryloyl analogue (−)-**1a**, this transition state is slightly higher in energy than that of the C(α)-*si*-face attack on the *anti*-s-*cis* conformer.

Table 2. *PM3 Values Calculated for the Cycloaddition of (−)-***1b** *to Cyclopentadiene* (see *Fig. 2*)

Conformer	ΔH_{form} [kcal/mol]	LUMO [eV]	C(α)-*re* at. coef.	C(β)-*re* at. coef.
syn-s-*trans*	–98.60	–0.479	–0.065	0.085
anti-s-*trans*	–99.60	–0.680	*0.055*	*–0.030*
syn-s-*cis*	*–101.18*	–0.405	*0.080*	*–0.060*
anti-s-*cis*	*–102.76*	–0.558	–0.030	0.035
Conformer	C(α)-*si* at. coef.	C(β)-*si* at. coef.	$\Delta H^{\neq}$ (C(α)-*re*) [kcal/mol]	$\Delta H^{\neq}$ (C(α)-*si*) [kcal/mol]
syn-s-*trans*	*0.105*	*–0.085*	–27.35	–30.13
anti-s-*trans*	–0.030	0.030	–28.90	–31.73
syn-s-*cis*	–0.050	0.055	*–33.12*	–32.70
anti-s-*cis*	*0.050*	*–0.045*	*–35.26*	*–33.18*

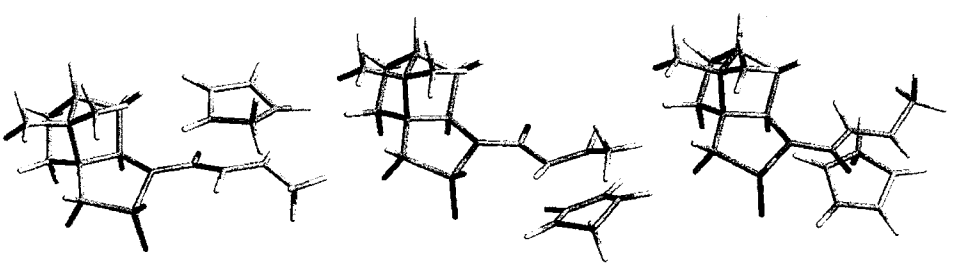

C(α)-*re anti*-s-*cis* C(α)-*si anti*-s-*cis* C(α)-*re syn*-s-*cis*

Fig. 2. *The three transition states participating to the stereochemical outcome of the cyclopentadiene addition to* (−)-**1b**

The third example discussed[17]) is the addition of cyclopentadiene to *N*,*N*′-fumaroyl-bis[bornanesultam] (−)-**1c**, reported to give 85% d.e. in favour of C(α)-*re*-face attack [14]. First of all, considering the conformational analysis, we see that both bis(*anti*-s-*cis*) and bis(*syn*-s-*cis*) conformers are the most stable, but that the *syn*-s-*cis*-s-*trans*-*syn* as well as the *syn*-s-*cis*-s-*cis*-*anti*, *anti*-s-*cis*-s-*trans*-*anti* and *syn*-s-*trans*-s-*cis*-*anti* nonsym-

[17]) Chronologically, to rationalize the experimental results [14], we started our calculations with this example. However, due to the size of (−)-**1c** and the resulting time-consuming problems, we turned our attention to **2b**, anticipated to be more promising. In view of the discrepancy observed between calculations and experimental results [7] (*vide infra*), we then systematically studied the other examples.

metrical conformations may also be present in solution (see *Table 3*). In view of the small conformational-energy differences and the supposed simplicity of their ^{1}H-NMR spectra, we attempted to analyse the conformational equilibrium by means of this method. Accordingly, the temperature was decreased stepwise (20 K) from 293 to 193 K in deuterated acetone, and the NMR coalescence temperature was found to be at 253 K. Spectral analysis at 193 K shows, for the olefinic protons, two *s* at 7.62 (95.32%) and 6.86 ppm (0.31%) besides two *AB* systems at 7.36 (J = 15 Hz, $\Delta\nu$ = 152.6 Hz; 4.08%) and 6.78 ppm (J = 12 Hz, $\Delta\nu$ = 44.0 Hz; 0.29%), suggesting, at this temperature, the presence of two symmetrical and two unsymmetrical species[18]). The degree of nonsymmetry is difficult to estimate, since a small difference in the torsional angles may result in differentiated *AB* signals for the protons at C(α) and C(α′). By virtue of the *Tolber*-and-*Ali* co-operative effect [30], the symmetrical, more stable bis(*anti*-s-*cis*) conformation should lead to a favoured transition state. According to the same principle, the bis(*syn*-s-*cis*) arrangement also benefits from the cumulative steric/stereoelectronic effects. Indeed, if C(α)-*re*-face attack on the bis(*anti*-s-*cis*) conformer is the most favoured, unexpectedly, the minor diastereoisomer seems to originate from C(α)-*si*-face attack on the bis(*syn*-s-*cis*) conformer. In parallel, C(α)-*re*-face attack on this conformer also contributes to the overall stereochemical outcome of this reaction with the combined unsymmetrical *syn*-s-*cis*-s-*cis*-*anti* conformer (see *Table 3*). In addition to the co-operative principle, the high

Table 3. *PM3 Values Calculated for the Cycloaddition of (−)-* **1c** *to Cyclopentadiene* (see *Fig. 3*)

Conformer	ΔH_{form} [kcal/mol]	LUMO [eV]	C(α)-*re* at. coef.	C(α′)-*re* at. coef.
bis(*syn*-s-*trans*)	–188.3	–1.127	*0.250*	*–0.269*
bis(*anti*-s-*trans*)	–191.1	–0.702	*0.130*	*–0.140*
syn-s-*cis*-s-*trans*-*anti*	–191.6	–1.099	*0.045*	*–0.060*
syn-s-*trans*-s-*trans*-*anti*	–192.2	–0.977	0.105	–0.105
syn-s-*trans*-s-*cis*-*anti*	*–195.0*	–0.993	–0.160	0.180
anti-s-*cis*-s-*trans*-*anti*	*–196.5*	–0.760	–0.190	0.206
syn-s-*cis*-s-*cis*-*anti*	*–196.6*	–0.874	–0.230	0.220
syn-s-*cis*-s-*trans*-*syn*	*–196.9*	–1.035	–0.235	0.225
bis(*syn*-s-*cis*)	*–196.9*	–0.976	*–0.260*	*0.255*
bis(*anti*-s-*cis*)	*–197.1*	–0.783	–0.201	0.190

Conformer	C(α)-*si* at. coef.	C(α′)-*si* at. coef.	$\Delta H^{\neq}$(C(α)-*re*) [kcal/mol]	$\Delta H^{\neq}$(C(α)-*si*) [kcal/mol]
bis(*syn*-s-*trans*)	–0.270	0.240	–121.67	–123.00
bis(*anti*-s-*trans*)	–0.135	0.125	–121.86	–124.99
syn-s-*cis*-s-*trans*-*anti*	–0.040	0.045	–128.13[a])	–130.60[a])
syn-s-*trans*-s-*trans*-*anti*	*–0.110*	0.105	–120.85[a])	–124.80[a])
syn-s-*trans*-s-*cis*-*anti*	*0.180*	*–0.190*	–127.20[a])	–129.90[a])
anti-s-*cis*-s-*trans*-*anti*	*0.210*	*–0.220*	–126.23[a])	–125.90[a])
syn-s-*cis*-s-*cis*-*anti*	*0.250*	*–0.240*	*–132.23*[a])	–129.58[a])
syn-s-*cis*-s-*trans*-*syn*	*0.240*	*–0.255*	–126.51[a])	–130.03[a])
bis(*syn*-s-*cis*)	0.240	–0.235	*–131.82*	*–131.27*
bis(*anti*-s-*cis*)	*0.206*	*–0.195*	*–133.15*	–129.57

[a]) For unsymmetrical conformers, both '*endo*' and '*exo*' transition states have been calculated. Only the most favourable is reported.

[18]) At 213 K, this ratio is 95.17:0.42:4.10:0.31.

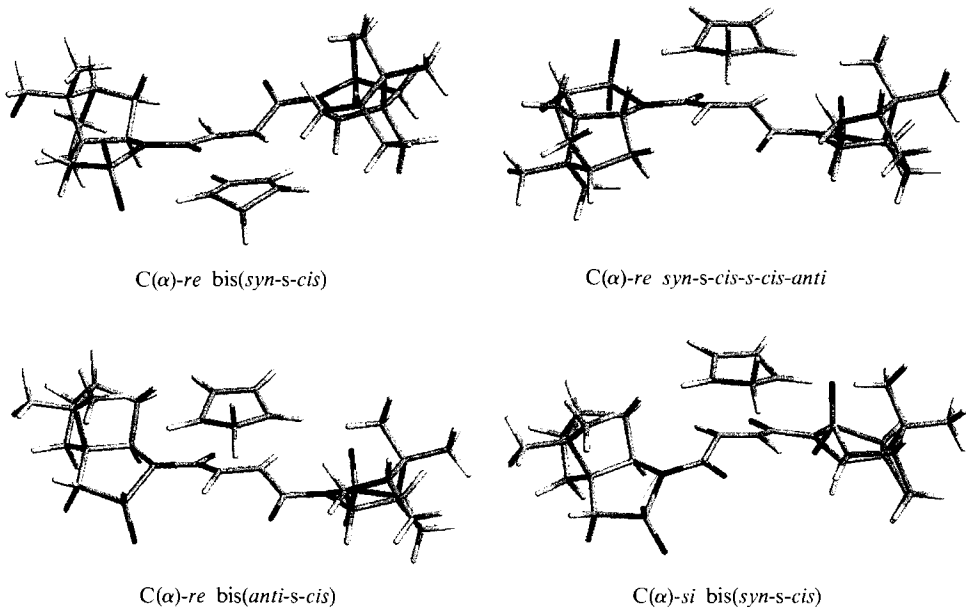

Fig. 3. *The four transition states participating to the stereochemical outcome of the cyclopentadiene addition to* (−)-**1c**

diastereoselectivity observed for (−)-**1c**, as compared to (−)-**1a**,**b**, is also a possible consequence of its favourable entropic term, not considered in the ΔH_{form} calculated by PM3. Fortunately, this uncatalyzed reaction was reported at two different temperatures (at −78°, 89% d.e. [14]), thus allowing us to calculate the overall activation-entropy difference, roughly estimated to be −2.3 cal/Kmol[19]).

The rigidity of the *N*-glyoxyloyl-bornanesultam hetero-dienophile **2a** is even less favoured in comparison with its analogue (−)-**1a**, due to the absence of the *cis*-positioned H−C(β), which restricts free rotation around the C(O)−C(α) bond. As a result, practically all four possible conformers of **2a** are present at room temperature and thus may also participate in the stereochemical outcome of the reaction, as indicated by the energies of the transition states (see *Table 4*), as well as by the global low diastereoselectivity observed (46% d.e. [31]). Six transition states contribute to *endo* addition, whereas five transition states may be responsible for *exo* addition. The most important contributors are the C(α)-*si endo* and *exo* cycloadditions to the *anti*-s-*cis* conformer[20]) (see *Fig. 4*). It is worthwhile to note that, under 8 kbar, the more compact C(α)-*re exo syn*-s-*cis* and

[19]) Statistically, three conformers participate in attack on the C(α)-*re* face, *vs.* only one for the C(α)-*si* face. Furthermore, for comparison, we performed the uncatalysed addition of cyclopentadiene in refluxing CH_2Cl_2 for 24 h to (−)-**1a** (94% yield, 86.5% *endo*, 46.2% d.e.), (−)-**1b** (80% yield, 76.4% *endo*, 36% d.e.), (−)-**1c** (98% yield, 81.6% d.e.), and (−)-**3b** (95% yield, 76.6% *endo*, 36% d.e.), thus allowing an estimation of their $\Delta\Delta S^{\neq}$ to −17.8, −10.8, −2.3, and −13.9 cal/Kmol, respectively.

[20]) Due to the heteroatom, the *re* and *si* nomenclature priority has changed.

C(α)-*re endo anti*-s-*trans* transition states are more favoured, thus increasing, in both cases, the two minor diastereoisomers by 2%, resulting in a decrease of the overall diastereoselectivity (38% d.e. [32])[21]).

Table 4. *PM3 Values Calculated for the Cycloaddition of* **2a** *to 1-Methoxybuta-1,3-diene* (see *Fig. 4*)

Conformer	*anti*-s-*cis*	*syn*-s-*cis*	*anti*-s-*trans*	*syn*-s-*trans*
Volume [Å^3]	223.3	*221.9*	225.2	224.5
ΔH_{form} [kcal/mol]	*–137.0*	*–135.0*	–134.7	*–135.1*
LUMO [eV]	–0.908	–0.745	–0.738	–0.730
C(α)-*re* atom. coef.	*0.061*	–0.055	–0.055	*–0.135*
O(β)-*re* atom. coef.	*–0.060*	0.085	0.085	*0.122*
C(α)-*si* atom. coef.	–0.035	*0.100*	*0.090*	0.110
O(β)-*si* atom. coef.	0.045	*–0.085*	*–0.075*	–0.121
$\Delta H^{\neq}$ (*endo*C(α)-*re*) [kcal/mol]	*–113.7*	*–113.6*	*–113.8*	*–113.2*
Volume$^{\neq}$ [Å^3]	308.3	308.2	*306.3*	307.1
$\Delta H^{\neq}$ (*endo*C(α)-*si*) [kcal/mol]	*–115.1*	*–113.6*	–110.4	–108.6
Volume$^{\neq}$ [Å^3]	309.4	308.2	309.9	309.5
$\Delta H^{\neq}$ (*exo*C(α)-*re*) [kcal/mol]	*–114.6*	*–114.3*	*–113.5*	–111.3
Volume$^{\neq}$ [Å^3]	308.4	*306.8*	308.5	307.9
$\Delta H^{\neq}$ (*exo*C(α)-*si*) [kcal/mol]	*–115.4*	*–113.5*	–111.6	–112.8
Volume$^{\neq}$ [Å^3]	308.8	306.9	309.3	307.8

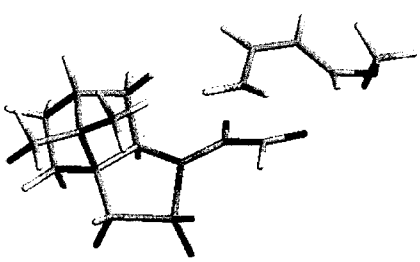

C(α)-*si endo anti*-s-*cis*

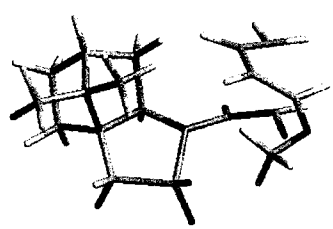

C(α)-*re endo anti*-s-*trans*

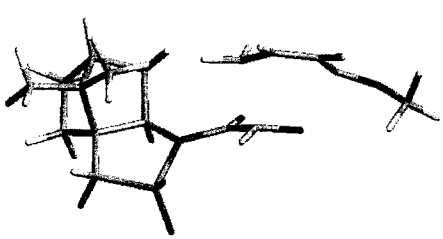

C(α)-*si exo anti*-s-*cis*

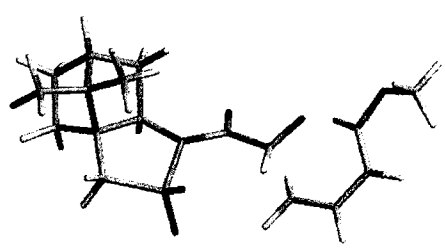

C(α)-*re exo anti*-s-*cis*

Fig. 4. *The four main transition states participating to the stereochemical outcome of the 1-methoxybuta-1,3-diene addition to* **2a**

[21]) At higher pressure, the C(O)–CHO s-*cis* conformation is preferred, as earlier reported [33] and calculated for *syn*- and *anti*-**2a** (*Table 4*).

The case of *N*-(acylnitroso)sultam **2b** is particularly interesting. Indeed, during the cycloaddition, the N-atom does not become a stereogenic centre, and thus for a same face, the *endo* and *exo* attack generate two different diastereoisomers. The complete diastereoselectivity, reported by *Ghosez* and coworkers, is thus extraordinary since it implies both total π-face and *endo*/*exo* selectivity [7]. We anticipated particularly important energy differences for the possible transition states. First of all, if the *anti*-s-*cis* and *syn*-s-*cis* conformers are the most stable (see *Table 5*), the differences of energy calculated

Table 5. *PM3 Values Calculated for the Cycloaddition of* **2b** *to Cyclopentadiene* (see *Fig. 5*)

Conformer	ΔH_{form} [kcal/mol]	LUMO [eV]	N(α)-*re* at. coef.	O(β)-*re* at. coef.	N(α)-*si* at. coef.
syn-s-*trans*	–84.7	–1.103	*–0.410*	*0.310*	0.320
anti-s-*trans*	–85.2	–1.024	–0.240	0.240	0.247
syn-s-*cis*	*–87.2*	–1.005	–0.330	0.340	*0.350*
anti-s-*cis*	*–89.2*	–0.931	*0.298*	*–0.265*	–0.290
Conformer	O(β)-*si* at. coef.	$\Delta H^{\neq}$ (*endo*-*re*) [kcal/mol]	$\Delta H^{\neq}$ (*endo*-*si*) [kcal/mol]	$\Delta H^{\neq}$ (*exo*-*re*) [kcal/mol]	$\Delta H^{\neq}$ (*exo*-*si*) [kcal/mol]
syn-s-*trans*	–0.340	*–13.91*	*–13.61*	–13.27	–12.16
anti-s-*trans*	–0.205	*–14.09*	*–13.64*	–11.45	–12.21
syn-s-*cis*	*–0.330*	*–13.92*	*–14.52*	–11.13	–12.98
anti-s-*cis*	0.235	*–15.20*	*–16.10*	*–14.63*	*–14.63*

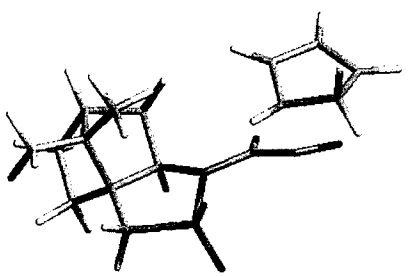

C(α)-*si endo anti*-s-*cis*

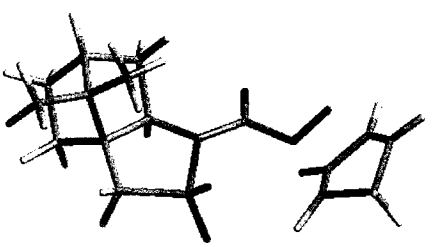

C(α)-*re endo anti*-s-*cis*

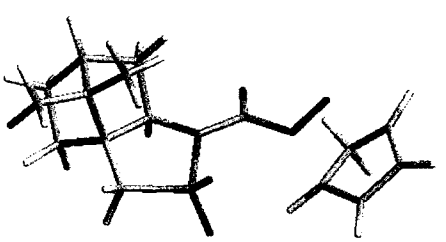

C(α)-*re exo anti*-s-*cis*

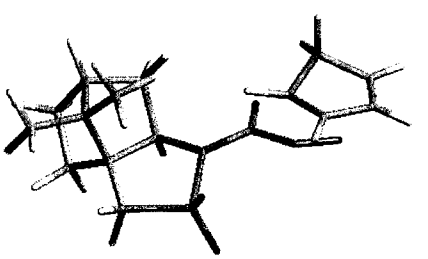

C(α)-*si exo anti*-s-*cis*

Fig. 5. *The four main transition states participating to the stereochemical outcome of the cyclopentadiene addition to* **2b**

for the *trans* conformers (4.0 and 4.5 kcal/mol) differ considerably from the reported values (19.7 and 34.5 kcal/mol [7]). Furthermore, according to our calculations, all eight possible *endo* as well as two *exo* transition states can contribute to the stereochemical outcome of this reaction. For example, the energy difference between the *endo-re* and *endo-si* approach is only 0.9 kcal/mol[20])[22]) (see *Table 5*).

At this point, we wondered if our calculations were correct and significant. We thus focused on the two most favourable s-*cis* conformations, by increasing the level of theory to the much more time-consuming STO 3-21G level. As shown in *Table 14* (see *Exper. Part*) for (–)-**1a,b** and **2a,b**, these *ab initio* calculations confirmed both the thermodynamic stability of the *anti*-s-*cis* and the high reactivity of the *syn*-s-*cis* conformers in terms of LUMO level and planarity of the N-atom. The stereoelectronic influence of the pyramidal N-atom on the LUMO is less pronounced than in the PM3 calculations. This is particularly the case for *syn*-s-*cis*-**2b** (*Table 14*) and results from a more planar N-atom as compared to the PM3 calculated geometries (see *Tables 9* and *10* for ΔhN comparison in *syn* and *anti* disposition). To validate this theoretical approach, we then decided to compare the theoretical models with experimental physical properties such as geometry, observed by X-ray analyses, and ionization energies, obtained by photoelectron spectroscopy (PES). With respect to the instability of **2a,b** and the necessity to have material volatile enough for PES analyses, we chose (–)-**1a,b,d**[23]) as probes, as well as for additional X-ray analyses, the s-*trans* disubstituted (–)-**1e** analogue and the *syn*-bornanesultam (–)-**2f** [34], obtained by ozonolysis of (–)-**1d,e** (O_3 in AcOEt at –78°, then Me_2S; 86–90%), and finally, (–)-**3b** as an example of a toluenesultam [35][24]).

First of all, we see in *Table 15* (see *Exper Part*), that AM1 calculations are unable to correctly treat the pyramidalization of the N-atom as well as the torsional angles observed in the crystalline state[25]). The superiority of the PM3 HOMO calculations, done on the thermodynamically most stable (–)-*anti*-s-*cis*-**1a,b** and (–)-*anti*-s-*trans*-**1d** conformers, becomes even more evident after comparison of the PES measurements (see *Fig. 6*). As a general trend, the PES analyses are always higher in energy than the theoretical values[26]). From the quantitative point of view, the best standard deviations are observed at the PM3 level of theory for both absolute or relative differences of energies. If the energy levels from the HOMO to the HOMO – 3 decrease regularly for the monosubstituted (–)-**1b,d**, it is noteworthy that for (–)-**1a**, the HOMO – 1 and HOMO – 2 are identical. This is again very well reflected by the PM3 calculations and thus persuaded us to pursue our investigations with this model.

---

[22]) Besides (–)-**1c** and **2a** which possess, in the transition states, similar distances for the two newly formed partial bonds, the other dienophiles (–)-**1a,b** and (–)-**3a,b** show generally a slightly larger distance for the C(α) as compared to the C(β) partial bonds. With the smallest N(α) (*ca.* 1.88 Å, see *Table 13*) as compared to the O(β) (*ca.* 2.13 Å) partial bonds, **2b** is an exception, suggesting an asynchronous cycloaddition [23].

[23]) We are indebted to Prof. *Curran* for communicating us the correct X-ray cell value for (–)-**1d** (a = 7.698(4) Å).

[24]) The X-ray structure analyses of (–)-**3b,e** will be published in due course [36a].

[25]) We are conscious that this is not a strong argument since, due to packing effects, geometries in the crystalline state may be different than in solution or in the gas phase. For comparison of semi-empirical methods with X-ray-structure analyses, see [36b].

[26]) Or lower when considering the positive ionization energies (see *Exper. Part*) instead of the negative values relative to the HOMO. The theoretical values were calculated for the more stable conformers as opposed to the experimental values, resulting from a conformational distribution.

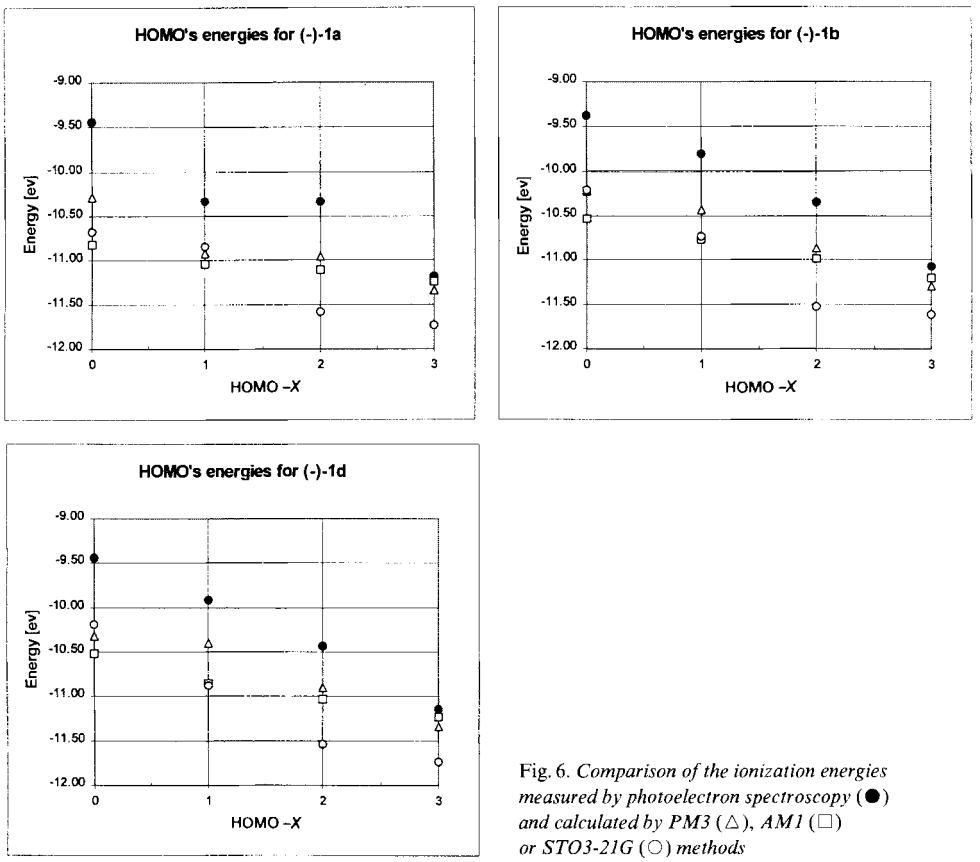

Fig. 6. *Comparison of the ionization energies measured by photoelectron spectroscopy* (●) *and calculated by PM3* (△), *AM1* (□) *or STO3-21G* (○) *methods*

Therefore, in view of the assumed correct PM3 results, we decided to repeat the cycloaddition of **2b** to cyclopentadiene. The commercially available bornane-10,2-sultam (+)-(2*S*)-**2c** was deprotonated (NaH, 1.2 equiv., toluene) and acylated with phosgene (20% solution in toluene, 1.1 equiv.) prior to treatment with $NH_2OH \cdot HCl$ (1.5 equiv.) and K_2CO_3 (3 equiv.) in wet Et_2O [37] (*Scheme*). Purification on SiO_2 afforded the desired precursor (+)-(2*S*)-**2e** in 20% yield, besides recovered (+)-(2*S*)-**2c** (63%)[27]). *In situ* oxidation with Et_4NIO_4[28]) (1.0 equiv.) in CH_2Cl_2 in the presence of cyclopentadiene (5.0 equiv.) according to *Ghosez*'s procedure, resulted, after 3 h at room temperature and ^{1}H-NMR analysis of the crude adduct (94% yield), in a 75.8:1.5:22.7 (2*S*,1′*S*,4′*R*)-**5a**/(2*S*,1′*R*,4′*S*)-**5a**/(2*S*)-**2c** mixture. Purification by chromatography (SiO_2) furnished pure (+)-(2*S*,1′*S*,4′*R*)-**5a** (50% yield) and (+)-(2*S*)-**2c** (13%). We were intrigued about the origin of the free sultam (+)-(2*S*)-**2c**. Supposing a possible selective hydrolysis[28]), we repeated the same cycloaddition in the presence of 4-Å molecular sieves and obtained a 81.3:4.0:14.7 mixture of the same three compounds in 92% yield. We then decided to prepare the diastereoisomer mixture by coupling the racemic oxazine salt **4a** (1 equiv.)

[27]) We are indebted to Prof. *Ghosez* for providing us, after submission of this manuscript, with the detailed Exper. Part of [7].

[28]) Commercially available Et_4NIO_4 contains *ca.* 10% (*w*/*w*) of H_2O. See also Footnote 20 in [34a].

with (2*S*)-**2d** (0.5 equiv.) and K_2CO_3 (1 equiv.) in wet Et_2O [37]. The 30.2:52.4:17.4 (2*S*,1′*S*,4′*R*)-**5a**/(2*S*,1′*R*,4′*S*)-**5a**/(2*S*)-**2c** mixture thus obtained (49% yield) was treated with Et_4NIO_4 (2.0 equiv.) in the absence of cyclopentadiene to give after 3 h, a 33.2:48.4:18.4 mixture and, after 72 h, a 37.3:43.8:18.9 mixture, clearly showing the diminution of the major signal in the ^{1}H-NMR analysis of the crude material[29]). Nevertheless, the signal of the free sultam (+)-(2*S*)-**2c** was not increasing proportionally[30]). For this reason, we also treated the precursor (+)-(2*S*)-**2e** with Et_4NIO_4 in the absence of cyclopentadiene and observed a very clean and complete hydrolysis after 3 h. A 55:35:10 diastereoisomer mixture of (2*S*,1′*S*,4′*R*)-**5a**/(2*S*,1′*R*,4′*S*)-**5a**/(2*S*)-**2c** was also treated with cyclohexadiene (5.0 equiv.) in the presence of Et_4NIO_4 (1.0 equiv.) to afford, after 12 h, a 32:28:17:14:9 mixture of (2*S*,1′*S*,4′*R*)-**5a**/(2*S*,1′*R*,4′*S*)-**5a**/(2*S*,1′*S*,4′*R*)-**5b**/(2*S*,1′*R*,4′*S*)-**5b**/(2*S*)-**2c**[31]). This control experiment demonstrates that one diastereoisomer more rapidly or selectively undergoes a *retro-Diels-Alder* reaction. The diene and dienophile thus regenerated may participate in a new cycloaddition, whose iterative nature can completely drive the reaction towards the most stable diastereoisomer (thermodynamic control[32])). This process proceeds in competition with hydrolysis of the transient hetero-dienophile **2b**. We performed a PM3 conformational minimization analysis by effecting a systematic drive of the two N–C(O) bonds for both diastereoisomers. The *anti*-(2*S*,1′*S*,4′*R*)-**5a** is thermodynamically more stable (−64.03 kcal/mol, $\Delta hN = 0.419$ Å) in a pseudo-*endo* conformation of the oxa-azabicycloheptene ring, as compared to its pseudo-*exo* conformer (−62.46 kcal/mol). In contrast, the *anti*-(2*S*,1′*R*,4′*S*)-**5a** is more stable in the pseudo-*exo* conformation (−62.96 kcal/mol, $\Delta hN = 0.449$ Å) as compared to its pseudo-*endo* arrangement (−62.58 kcal/mol). Both N-atoms in the cycloadducts are pyramidal, and, resulting from the oxa-aza-bicyclo[2.2.1]geometry, the pseudo-*exo* diastereoisomer (2*S*,1′*R*,4′*S*)-**5a** possesses the most pyramidalized N-atom[33]). As a consequence, this one is the most destabilized by the *syn*-periplanar N and O lone pairs, and thus, could be prone to stereoelectronically assisted selective *retro-Diels-Alder* reaction or/and hydrolysis[34]). This may well explain the divergences between the calculated and experimental results.

[29]) A chromatographically purified 40.0:57.4:2.6 mixture was similarly treated under the same conditions to give a 51.7:40.1:8.2 mixture after 15 h. The process was accelerated in the presence of additional H_2O (2.0 equiv.) to give, after 3 h, a 44.2:43.4:12.4 mixture. Alternatively, a 55:35:10 mixture was treated with cyclopentadiene (5.0 equiv.) in refluxing CH_2Cl_2 in the absence of oxidant, to afford a 68:22:10 mixture after 3 h.

[30]) Furthermore, the free oxazine is unstable [38a] and could neither be isolated nor detected in the reaction mixture.

[31]) Absolute configurations are based on the chemical correlation reported by *Ghosez* and coworkers [7].

[32]) This may also be the case for **2a**, in view of the reported time-dependent diastereoselectivity [31] [32]. We controlled that the diastereoisomer ratios for cycloadducts derived from homo-dienophiles (−)-**1a**,**b**,**c** or (−)-**3a**,**b** and cyclopentadiene remain unchanged after refluxing 24 h in $CHCl_3$ with cyclohexadiene, thus indicating a kinetic control.

[33]) Furthermore, as a result of the generalized anomeric effect [39], the sultam N lone pair imparts a dissymmetry to the carbonyl π-orbitals, which may also interfere with the oxazine N lone pair. According to PM3 calculations for (−)-**1**,**2**,**3a**,**b**, this dissymmetry is also perceptible on the C(O) LUMO atomic coefficients, which are both more important on the face of the N lone pair, thus resulting in a favourable second-order MO overlap for the *anti*-s-*cis* conformers.

[34]) This may not be excluded under these conditions. For anhydrous oxidative conditions, see [38b]. The case of **5b** is different. The enthalpies of formation, expressed in kcal/mol, were calculated and are the following: pseudo-*endo* (2*S*,1′*S*,4′*R*)-**5b**, −84.39, $\Delta hN = 0.44$ Å; pseudo-*exo* (2*S*,1′*S*,4′*R*)-**5b**, −83.35; pseudo-*endo* (2*S*,1′*R*,4′*S*)-**5b**, −83.87; pseudo-*exo* (2*S*,1′*R*,4′*S*)-**5b**, −85.33, $\Delta hN = 0.387$ Å.

Scheme

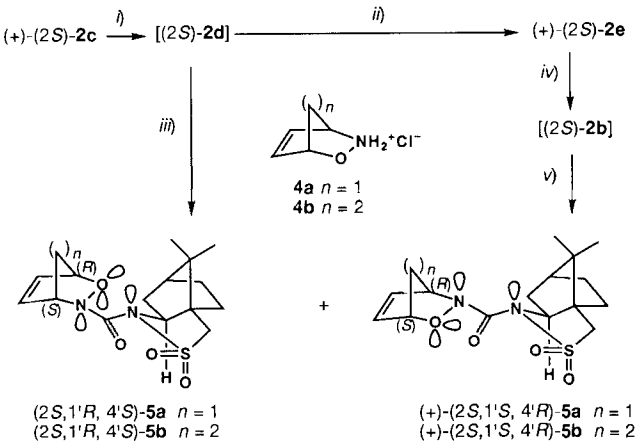

i) NaH, toluene, $C(O)Cl_2$. *ii*) $NH_2OH \cdot HCl$, K_2CO_3, Et_2O (20% from (+)-**2c**). *iii*) K_2CO_3, Et_2O (49%). *iv*) Et_4NIO_4, CH_2Cl_2. *v*) Cyclopentadiene (50%).

In his quest to gain a deeper understanding on the origin of diastereoselectivity when using (−)-**2c** as a chiral auxiliary, *Oppolzer* and coworkers designed the structurally simpler toluenesultams (+)-**3c,d**, possessing a single stereogenic centre instead of the bornane skeleton [35] [40]. These new chiral auxiliaries were also speculatively compared to a 2,5-dimethylpyrrolidine system by *Kim* and *Curran* [9]. The thermal cycloaddition of (−)-**3a** to cyclopentadiene led to 62% d.e. in the *endo* (96%) attack, and the authors were surprised to observe that, in the presence of 1 equiv. of chelating $TiCl_4$, the π-facial selectivity dropped to 11% d.e. [35a]. It was only in the presence of 2 equiv. of *Lewis* acid that the diastereoselectivity could be increased ($EtAlCl_2$, −78°, 91% d.e., 99% *endo*) [35a]. Furthermore, contrary to their expectations, the sterically more demanding *t*-**Bu** analogue (−)-**3b** was even less effective in the thermal (room temperature, 51% d.e., 80% *endo*) and *Lewis*-acid-promoted additions ($EtAlCl_2$, −78°, 77% d.e., 95% *endo*) [35a].

PM3 Calculations help us to understand these results for the thermal cycloadditions. Accordingly, C(α)-*re*-face attacks on the more abundant *anti*-s-*cis* and thermodynamically less favoured *syn*-s-*cis* conformers are believed to be responsible for the diastereoselection observed (see *Table 6*). The minor diastereoisomer is thought to result mainly from C(α)-*si*-face attack on the minor *syn*-s-*cis* conformer for (−)-**3a** (*Table 6*). The situation is different for (−)-**3b**, where both C(α)-*re* and C(α)-*si*-face attacks occur on the *anti*-s-*cis* conformer, whilst, at room temperature, the *syn*-s-*cis* conformer is mainly responsible for the C(α)-*re*-face selectivity (see *Table 7*). We note that this model may also tentatively explain the *Lewis*-acid-mediated reactions. Indeed, for (−)-**3a**, the energy difference between the C(α)-(*re*) and C(α)-*si* approach is extremely small (0.19 kcal/mol) for a *syn*-s-*cis* conformation, corresponding to the mono-chelated case, when compared to either the thermal addition (0.37 kcal/mol) or the purely *anti* arrangement, hypothetically corresponding to the non-chelating SO_2 and C(O) di-coordination in the presence of 2 equiv. of *Lewis* acid[35]).

[35]) Assuming that the *Lewis*-acid ligands do not interfere in the π-facial shielding [27], which is not obvious in view of possible non-chelating out-of-plane complexation [26].

Table 6. *PM3 Values Calculated for the Cycloaddition of (−)-***3a** *to Cyclopentadiene* (see *Fig. 7*)

Conformer	ΔH_{form} [kcal/mol]	LUMO [eV]	C(α)-*re* at. coef.	C(β)-*re* at. coef.
syn-s-*trans*	–57.1	–0.708	0.0060	–0.0095
anti-s-*trans*	–56.4	–0.844	*–0.0085*	*0.0070*
syn-s-*cis*	*–59.9*	–0.695	*–0.0090*	*0.0100*
anti-s-*cis*	*–60.7*	–0.771	0.0030	–0.0065
Conformer	C(α)-*si* at. coef.	C(β)-*si* at. coef.	$\Delta H^{\neq}$(C(α)-*re*) [kcal/mol]	$\Delta H^{\neq}$(C(α)-*si*) [kcal/mol]
syn-s-*trans*	*–0.0075*	*0.0090*	9.85	9.71
anti-s-*trans*	0.0055	–0.0080	9.85	6.93
syn-s-*cis*	0.0050	–0.0085	*4.42*	*4.61*
anti-s-*cis*	*–0.0055*	*0.0070*	*4.24*	*4.80*

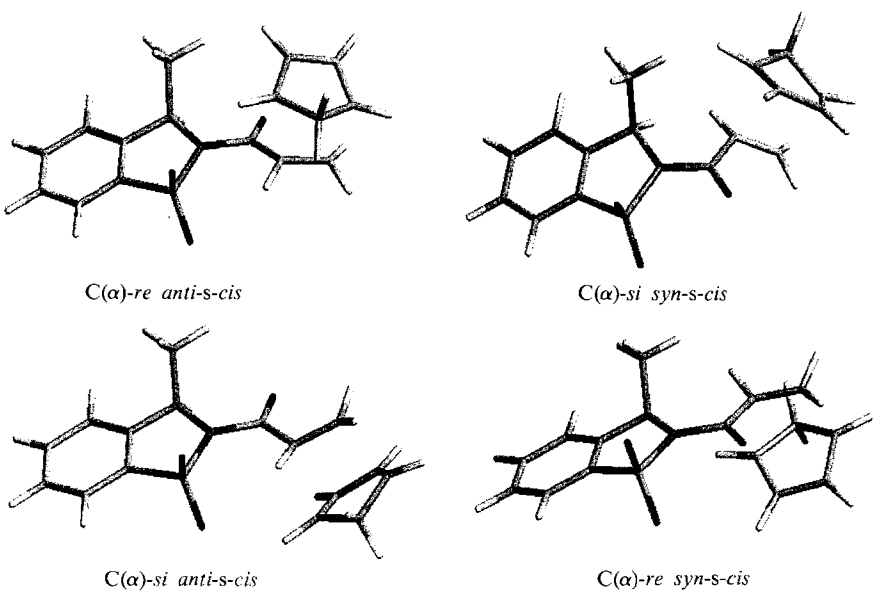

Fig. 7. *The four transition states participating to the stereochemical outcome of the cyclopentadiene addition to* (−)-**3a**

Table 7. *PM3 Values Calculated for the Cycloaddition of (−)-***3b** *to Cyclopentadiene* (see *Fig. 8*)

Conformer	ΔH_{form} [kcal/mol]	LUMO [eV]	C(α)-*re* at. coef.	C(β)-*re* at. coef.
syn-s-*trans*	–67.4	–0.692	–0.0075	0.0120
anti-s-*trans*	–65.8	–0.819	0.0125	–0.0130
syn-s-*cis*	*–70.5*	–0.679	*0.0110*	*–0.0140*
anti-s-*cis*	*–70.9*	–0.737	–0.0060	0.0100
Conformer	C(α)-*si* at. coef.	C(β)-*si* at. coef.	$\Delta H^{\neq}$(C(α)-*re*) [kcal/mol]	$\Delta H^{\neq}$(C(α)-*si*) [kcal/mol]
syn-s-*trans*	*0.0130*	*–0.0130*	–0.55	–1.94
anti-s-*trans*	–0.0075	0.0140	–1.41	–2.14
syn-s-*cis*	–0.0060	0.0130	*–5.09*	*–4.21*
anti-s-*cis*	*0.0075*	*–0.0110*	*–6.24*	*–5.07*

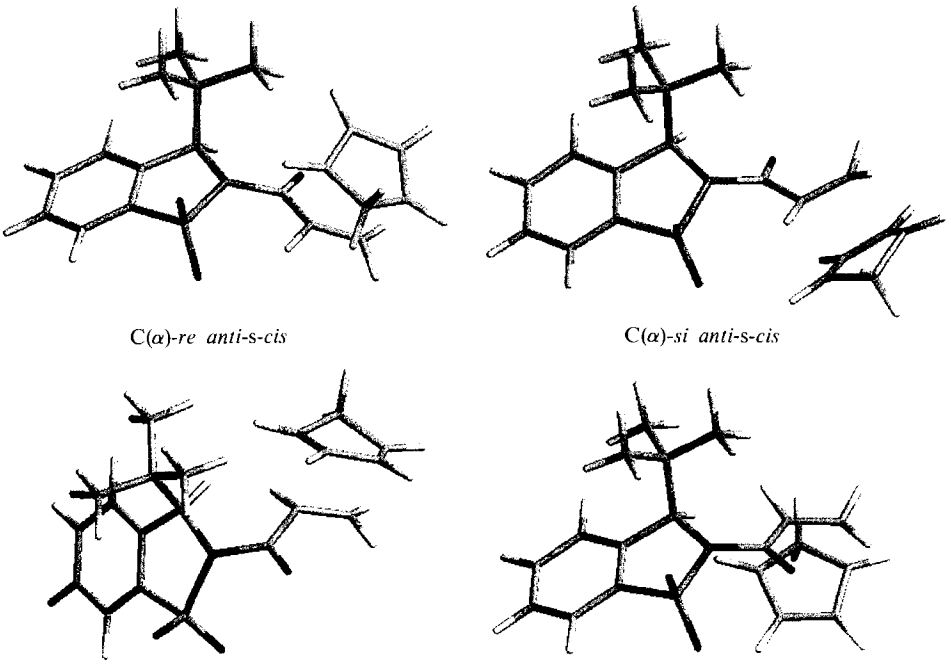

Fig. 8. *The four transition states participating to the stereochemical outcome of the cyclopentadiene addition to* **3b**

A possible explanation may be found in the orientation of the S=O(2) and alkyl groups as shown by the dihedral angles measured from the X-ray analyses of the dienophiles[24]) and cycloadducts [15] (see *Exper. Part, Table 18*) or from the geometry of the transition states (see *Exper. Part, Tables 16* and *17*). We clearly see that the bornane skeleton systematically induces, because of its intrinsic geometrical properties and the steric influence of the Me(8), a pseudo-equatorial orientation for both the C(3) and O(2) atoms, as well as the *N*-acyl substituent, in dienophiles derived from (−)-**2c**. In contrast, due to the *gauche* effect of the aromatic moiety, these atoms have a tendency to become both pseudo-axial[36]), especially for a large alkyl group such as in (−)-**3b**, thus losing the C_2 symmetrical properties of a 2,5-dimethylpyrrolidine system. As a consequence, the stereoelectronic influence is no longer mismatching the steric effect in the *anti*-s-*cis* conformation of (−)-**3b**. We initially thought that the π-facial stereoelectronic difference would be a direct consequence of the pseudo-axial groups, assuming that an axial H–C(2) bond has a more important influence than an axial C(3)–C(2) bond [41] in term of *Cieplak*'s theory [42][37]). Nevertheless, the stereoelectronically favoured face is system-

[36]) This tendency is even more pronounced in the absence of S=O(1) substitution. For example, the X-ray analysis of a cyclic sulfinamide [40] shows the following torsional angles: O(2)=S–N–C(2) −84.6°, S–N–C(2)–C(3) 99.2°. For convenience, the atom labels in **3** are the same as in **1** and **2**.

[37]) For sterically unbiased stereoelectronically controlled *Diels-Alder* reactions, see [43]. For studies refuting this theory by using 3-21G or AM1, see [44]. For rationalizations based on steric/torsional or electrostatic effects, see [45] [46], respectively. For matching/mismatching steric *vs.* electronic effects, see [47].

atically opposite to the N lone pair (lp) rather than the axial substituents. On the other hand, we assume that pyramidalization, hence the direction of the N-atom lone pair, is also influenced by an anomeric stabilization with the pseudo-axial O(1)=S bond in (−)-**2c** derivatives[38]). This anomeric effect [39] is in competition with steric interactions for toluenesultams. Indeed, such a stabilization would direct the large R^2 group s-*cis* to both O(2) and C(3) substituents, resulting in an unfavourable steric repulsion. It is noteworthy that, according to X-ray analysis [15], the pyramidalization is less pronounced or even inverted for toluenesultam derivatives, as compared to bornanesultams[39]). The high reactivity of the *syn*-s-*cis* conformer is partially due to the matching stereoelectronic/steric effects but more generally to a geometrically favoured more planar N, due to the *Coulomb*, steric, dipole-dipole SO_2/C(O) repulsions, resulting in a better electronic delocalization of the π-dienophilic system[40])[41]). Examination of the *Cambridge Structural Data Base* indeed shows that the pyramidalization in *N*-acylbornane-10,2-sultam derivatives is generally dependent on the S–N–C=O torsional angle (see *Fig. 9*). This dihedral angle, statistically determined to be around 153°, ranges from *ca.* 135 to 170° with a ΔhN height decreasing from *ca.* 0.350 to 0.150 Å, respectively. A pure *anti*-periplanar conformation is nevertheless difficult to reach due to the strong steric repulsion of the pseudo-

---

[38]) Although comparison of the O(1)=S–N–lp torsional angle and the O(1)=S or S–N interatomic distances did not reveal any obvious or systematic correlation [34].

[39]) See, *e.g.*, cycloadducts (+)-**7c** and (−)-**9** (numbering of the X-ray structures reported in [15]) with ΔhN = 0.035 and −0.061 Å, respectively (see *Table 18*). Thus, in the latter case, the N lone pair is oriented *anti*-periplanar to the pseudo-axial S=O(2) bond. The unsubstituted sultam (+)-**3c** shows an inverted pyramid with the most polarized N–H bond *anti*-periplanar to the pseudo-axial S=O(1) [40]. The O(1)=S–N–H torsional angle for the form A is −159°, corresponding to a possible σ^*–π stabilization, while form B corresponds to a possible anomeric stabilization with an O(2)=S–N–lp torsional angle of 164.7° as compared to O(1)=S–N–lp dihedral angles of −157.8, −153.5, −151.1, and −144.6° for (−)-**1a**,**b**,**d**,**e**, respectively. This may result from the fact that (+)-**3c** is an intermediate case, because the *gauche* effect exerted by the aromatic ring on the Me substituent is not strong enough to tip up alone the O(2) and C(3) atoms in a pseudo-axial direction. By virtue of symmetry, the N-atom, in noncyclic sulfonamides, remains planar [48a] or pyramidal [48b–d] with a lone pair bisecting the O=S=O angle. This has been rationalized as the result of a maximum delocalization over a sulfonamide linkage [49].

[40]) For the first example of a crystalline (−)-**2c** derivative in a non-chelated *syn* form, see [34a]; for the first example of a $TiCl_4$-chelated dienophile derived from (−)-**2c**, see [27]. The fractional coordinates of another apparent *syn*-*N*-acylbornane-10,2-sultam derivative are and stay unavailable [50].

[41]) It is noteworthy that, in their study on the origin of the diastereoselectivity in the [3+2] cycloadditions to (−)-**1a**, *Kim et al.* exclusively considered the *anti*-s-*cis* conformer, which possesses reduced atomic coefficients, and thus may have artificially minimized the influence of the third term to the advantage of the *Coulomb* term, despite a systematic drive of their transition states around the N–C(O) and C(O)–C(α) bonds [28]. The stereoselectivity reported for the [3+2] cycloaddition of acetonitrile oxide to (−)-**3b** [35b] may also partially be explained in terms of steric, stereoelectronic and *Coulomb* effects, by *C*(α)-*re* attack on the *syn*-s-*cis* conformer ($\Delta H^{\neq}_{form} = -13.09$ kcal/mol, δ(O(1)···O(dip)) = 4.36 Å, δ(O(2)···O(dip)) = 5.73 Å as compared to $\Delta H^{\neq}_{form} = -13.33$ kcal/mol, δ(O(1)···O(dip)) = 5.27 Å, δ(O(2)···O(dip)) = 4.99 Å for the *anti*-s-*cis* conformer [28]). With respect to the conformational energy of dipolarophile (−)-**3b**, the *syn*-s-*cis* conformer appears to be the most reactive species; furthermore, in view of the tiny enthalpic differences in the transition states, the entropy term, even though very small [28], could have a non-negligible impact. The situation is similar for acetonitrile-oxide addition to (−)-**1a** [10] (C(α)-*re* attack on *syn*-s-*cis* conformer, with $\Delta H^{\neq}_{form} = -33.56$ kcal/mol, δ(O(1)···O(dip)) = 4.44 Å, and δ(O(2)···O(dip)) = 5.77 Å, as compared to $\Delta H^{\neq}_{form} = -34.53$ kcal/mol, δ(O(1)···O(dip)) = 5.52 Å, and δ(O(2)···O(dip)) = 4.57 Å for the *anti*-s-*cis* conformer [28]).

equatorial C(3) atom, and the *ΔhN* height seems to reach a minimum of *ca.* 0.150 Å for angles larger than 160°. On the other hand, *syn*-periplanarity, where the C(O) is bisecting the O=S=O angle (S–N–C=O = –9.3°, *ΔhN* = 0.083 Å [34a]), is energetically possible with respect to the less demanding electrostatic and dipole-dipole repulsions[42]).

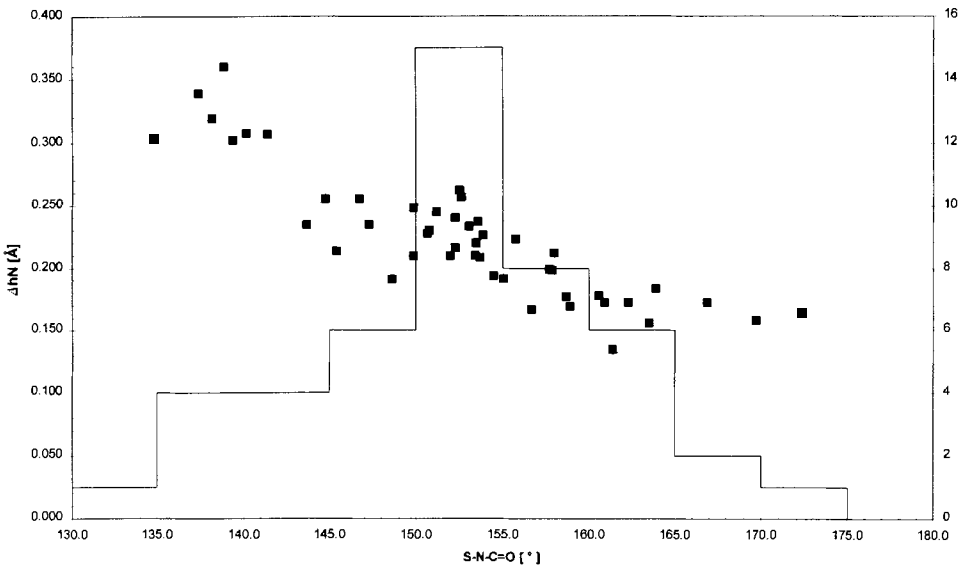

Fig. 9. *Population distribution of S–N–C=O dihedral angle in* N-*acylbornane-10,2-sultam derivatives and relationship with respect to Δ*hN *height*

Conclusion. – Semi-empirical PM3 calculations[43]) suggest that, in all seven examples of [4+2] thermal cycloadditions reported in the literature for *N*-acyl-bornanesultam or *N*-acyltoluenesultam-derived dienophiles, the thermodynamically and dipole-dipole favoured *anti*-s-*cis* conformers [10] [27] possess the lowest transition state, but that, in all instances, the *syn*-s-*cis* conformer also contributes to the stereochemical outcome of the reaction. The high reactivity of this conformer is partially due to the matching steric and electronic effects, but more generally to the less pyramidalized N-atom, which favours delocalization of the π-system. The more planar N-atom in the thermodynamically less favoured *syn* conformation is a geometrical consequence of steric, electrostatic and dipole-dipole repulsions between the SO_2 and C(O) groups. The attack of the diene, on the face opposite to the N lone pair, is stereoelectronically favoured. This results from the generalized anomeric effect of the N lone pair which dissymmetrizes the LUMO in particular, but more generally the MO and the π-system[44]). The direction of the N lone

[42]) The S–N–C=O torsional angle varies from 138 to 167° in the reactive *anti* transition states and from –25 to +6° in the reactive *syn* transition states (see *Exper. Part*, *Tables 9–13*, *16* and *17*).

[43]) The standard error of the PM3 method is ± 2 kcal/mol. We assume, for conformers or transition states, a constant error and thus correct relative and qualitative estimations.

[44]) For a review on the original concept of 'banana'-bond theory, see [51].

pair in *N*-acyl derivatives depends, in the absence of major steric restrictions, on a possible anomeric stabilization with the *anti*-periplanar S=O bond. For the dienes studied, only the hetero-dienophiles **2a,b** seem to react also in an *anti*-s-*trans* conformation, as proposed by *Pindur* and coworkers [6]. The recent concept of the stereoelectronic differentiating effect in *syn*-sultam derivatives, although in this case, apparently, of lower intensity as compared to the steric effect, may be extended to nucleophilic additions[45]) of **2,3c** derivatives. Finally, cyclopentadiene addition to **2b** was shown to be thermodynamically controlled. We hope that this discussion of the stereoelectronic contribution will help to a better understanding in the rationalization of other chemical transformations and in the design of new chiral auxiliaries.

This project was initiated by the publication of [53]. We are indebted to Prof. *A. Eschenmoser*, *A. Zamojski*, and *M. J. Kurth* for stimulating discussions. Prof. *N. Harada*, *J. Jurczak*, *H. J. Schaefer*, *E. Steckhan*, *E. Urban*, and *Y. Yamamoto* are thanked for providing us with X-ray fractional coordinates, as is Dr. *G. Bernardinelli* for his help in their analyses. We thank also Prof. *D. P. Curran* and *N. G. J. Richards* for helpful comments on the manuscript, as well as Prof. *E. Haselbach* for PES and Mr. *R. Brauchli* for low-temperature NMR analyses.

Experimental Part

General. See [54]. PES Analyses: *Turner*-type PES *Perkin-Elmer-PS16* model; He 21.22 eV (584 Å) with a resolution of 35 meV, using Ar (15.759 eV) as drift control; ionization potentials [eV]: (–)-**1a** (146°): 9.44, 10.34, 10.34, 11.18; (–)-**1b** (150°): 9.37, 9.81, 10.35, 11.07; (–)-**1d** (110°): 9.44, 9.91, 10.43, 11.14; (–)-**2f** (100°): 9.25, 9.73, 10.53, 11.53; (–)-**3b** (95°): 9.35, 9.85, 10.25, 10.98. X-Ray fractional coordinates obtained from the *Cambridge Structural Data Base* were analysed with Macro-Model program version 5.1 [55] on a *Silicon Graphics* work station *Indigo 2*. Selected values are reported in *Table 8*. PM3, AM1, and STO 3-21G calculations were performed on the same computer using the program Spartan version 4.1.1 [81]. Reported atomic coefficients correspond to the highest iso-value measured in the LUMO density volume. Selected torsional angles and distances for dienophile conformers and transition states are reported in *Tables 9–13*, *16* and *17*. A single imaginary frequency was obtained for each of the transition states. Further data are given in *Tables 14*, *15* and *18*.

Table 8. *X-Ray Fractional Coordinates Obtained from the* Cambridge Structural Data Base

ΔhN [Å]	S–N–C=O [°]	Ref.	*ΔhN* [Å]	S–N–C=O [°]	Ref.	*ΔhN* [Å]	S–N–C=O [°]	Ref.
0.135	161.4	[56]	0.199	157.7	[35]	0.237	153.6	[64]
0.156	163.5	[57]	0.208	153.7	[69]	0.240	152.3	[76]
0.158	169.7	[58]	0.210	149.9	[70]	0.245	151.2	[73]
0.164	172.4	[59]	0.210	152.0	[71]	0.248	149.9	[73]
0.167	156.7	[52]	0.210	153.4	[72]	0.255	144.8	[77]
0.169	158.9	[60]	0.212	158.0	[57]	0.255	146.7	[73]
0.172	160.9	[61]	0.214	145.4	[35]	0.257	152.6	[78]
0.172	162.3	[62]	0.216	152.3	[73]	0.262	152.5	[66]
0.172	166.9	[63]	0.220	153.5	[74]	0.302	139.4	[55]
0.177	158.7	[64]	0.223	155.8	[35]	0.304	134.8	[16]
0.178	160.6	[65]	0.226	153.9	[10]	0.307	141.4	[79]
0.183	163.9	[66]	0.228	150.7	[34]	0.308	140.2	[5]
0.191	148.6	[10]	0.230	150.8	[5]	0.319	138.2	[50]
0.191	155.1	[65]	0.233	153.1	[74]	0.339	137.4	[74]
0.193	154.5	[68]	0.235	143.7	[75]	0.360	138.9	[80]
0.198	157.9	[6]	0.235	147.3	[70]			

[45]) We have not studied this influence on the HOMO. For an alternative rationalization based on O(1) *vs.* O(2) chelation of the *syn*-enolate during electrophilic additions, see [52].

Table 9. *PM3 Values Calculated for the Cycloaddition and Transition States of (−)-***1a** *to Cyclopentadiene*

Conformer	S–N–C=O [°]	O=C–C=C [°]	ΔhN [Å]	HOMO [eV]	Trans.st.	S–N–C=O [°]	O=C–C=C [°]	δ(C(α)–C) [Å]	δ(C(β)–C) [Å]	O(1)=S–N–C(2) [°]	O(2)=S–N–C(2) [°]	S–N–C(2)–C(3) [°]	S–N–C(2)–H [°]	Imag. freq. [cm^{-1}]
					C(α)-*re*	−45.5	−160.4	2.20	2.09	106.8	−120.0	135.3	−102.0	873.38
syn-s-*trans*	−27.1	161.5	0.029	−10.214										
					C(α)-*si*	−30.1	151.4	2.22	2.07	105.3	−120.7	136.6	−99.5	865.15
					C(α)-*re*	169.2	−170.6	2.22	2.07	106.4	−121.7	135.9	−100.4	864.66
anti-s-*trans*	−176.4	−157.2	0.230	−10.323										
					C(α)-*si*	−131.2	97.4	2.22	2.07	97.4	−131.2	144.7	−90.6	866.09
					C(α)-*re*	−25.1	−1.7	2.23	2.07	103.6	−121.8	136.8	−99.5	860.64
syn-s-*cis*	−14.9	0.5	0.122	−10.215										
					C(α)-*si*	5.2	9.4	2.23	2.06	96.7	−128.1	142.1	−93.0	858.8
					C(α)-*re*	135.7	0.8	2.23	2.07	101.3	−127.7	140.8	−94.7	859.98
anti-s-*cis*	158.5	−2.2	0.152	−10.295										
					C(α)-*si*	157.3	13.3	2.25	2.06	105.2	−124.5	137.6	−98.4	835.11

Table 10. *PM3 Values Calculated for the Cycloaddition and Transition States of (−)-***1b** *to Cyclopentadiene*

Conformer	S–N–C=O [°]	O=C–C=C [°]	ΔhN [Å]	HOMO [eV]	Trans.st.	S–N–C=O [°]	O=C–C=C [°]	δ(C(α)–C) [Å]	δ(C(β)–C) [Å]	O(1)=S–N–C(2) [°]	O(2)=S–N–C(2) [°]	S–N–C(2)–C(3) [°]	S–N–C(2)–H [°]	Imag. freq. [cm^{-1}]
					C(α)-*re*	−45.8	−161.6	2.17	2.13	106.8	−119.7	135.3	−101.9	864.00
syn-s-*trans*	−27.5	161.9	0.015	−10.175										
					C(α)-*si*	−30.3	146.8	2.20	2.12	105.3	−120.7	136.5	−99.7	848.21
					C(α)-*re*	82.1	170.5	2.20	2.12	100.1	−128.5	142.1	−93.4	846.83
anti-s-*trans*	142.2	171.7	0.171	−10.264										
					C(α)-*si*	130.0	−172.5	2.18	2.11	96.2	−133.4	144.7	−90.9	854.70
					C(α)-*re*	−25.7	−3.2	2.19	2.11	103.8	−121.7	136.7	−99.6	860.43
syn-s-*cis*	−14.7	−0.1	0.119	−10.198										
					C(α)-*si*	−11.8	21.6	2.19	2.11	102.1	−122.9	137.8	−98.0	856.55
					C(α)-*re*	136.3	−1.4	2.19	2.11	101.2	−127.8	140.9	−94.7	859.84
anti-s-*cis*	158.3	−2.3	0.123	−10.228										
					C(α)-*si*	152.9	26.5	2.20	2.11	102.5	−126.6	139.4	−96.5	845.30

Table 11. *PM3 Values Calculated for the Cycloaddition and Transition States of (−)-* **1c** *to Cyclopentadiene*

Conformer	S–N–C=O [°]	O=C–C=C [°]	HOMO [eV]	Trans.st.	S–N–C=O [°]	O=C–C=C [°]	δ(C(α)–C) [Å]	O(1)=S–N–C(2) [°]	O(2)=S–N–C(2) [eV]	S–N–C(2)–C(3)	S–N–C(2)–H [°]	Imag. freq. [cm^{-1}]
				C(α)-*re*	−66.0, −44.3	−130.7, −165.6	2.14, 2.19	100.5, 104.0	−128.4, −123.4	141.0, 138.2	−94.2, −98.5	807.20
bis(*syn*-s-*trans*)	−25.1, −25.2	174.5, 174.5	−10.418									
				C(α)-*si*	−36,2, −43.6	−177.4, −174.9	2.16, 2.17	107.7, 106.1	−119.2, −121.4	135.0, 136.5	−100.6, −99.2	789.55
				C(α)-*re*	119.6, 135.1	−169.6, −139.9	2.18, 2.15	95.6, 104.0	−135.1, −124.7	144.9, 139.2	−90.4, −96.7	813.12
bis(*anti*-s-*trans*)	141.3, 142.2	169.2, 169.7	−10.292									
				C(α)-*si*	121.3, 134.6	179.9, −176.7	2.17, 2.14	102.2, 95.4	−126.8, −133.6	139.4, 145.0	−96.0, −90.6	818.16
				C(α)-*re*	−18.2, 83.6	−1.8, −160.3	2.17, 2.16	103.9, 91.7	−121.7, −137.3	136.6, 148.5	−99.6, −86.6	803.34
syn-s-*cis*-s-*trans*-*anti*	−26.0, −173.3	−6.6, −162.3	−10.078									
				C(α)-*si*	−5.4, 122.4	12.1, −171.1	2.16, 2.15	100.4, 96.8	−124.7, −132.1	139.6, 145.7	−95.4, −89.8	816.91
				C(α)-*re*	−49.1, 119.2	−157.5, −173.4	2.13, 2.19	106.0, 95.4	−120.6, −135.8	135.7, 144.9	−101.5, −90.4	804.12
syn-s-*trans*-s-*trans*-*anti*	−25.1, 141.5	155.4, 169.4	−10.156									
				C(α)-*si*	−39.2, 124.9	164.1, −170.6	2.14, 2.18	107.5, 99.2	−119.7, −131.3	135.3, 142.5	−100.4, −93.0	798.53
				C(α)-*re*	−44.7, 139.6	−163.2, −6.0	2.13, 2.20	108.0, 101.3	−119.2, −128.8	135.0, 141.5	−101.9, −93.9	824.99
syn-s-*trans*-s-*cis*-*anti*	−26.0, 158.7	160.8, −0.4	−10.192									
				C(α)-*si*	−42.0, 142.8	172.7, 27.4	2.16, 2.17	108.3, 99.7	−119.3, −129.8	134.7, 142.2	−100.6, −93.3	782.47
				C(α)-*re*	135.1, −72.0	−3.2, 177.7	2.17, 2.16	100.6, 105.4	−128.5, −124.5	141.6, 138.2	−93.8, −97.7	793.73
anti-s-*cis*-s-*trans*-*anti*	146.5, 124.4	−12.4, 151.5	−10.312									
				C(α)-*si*	106.4, 130.0	19.1, −174.1	2.15, 2.18	99.9, 96.8	−129.9, −133.5	141.7, 144.1	−93.7, −91.4	791.58
				C(α)-*re*	−25.4, 139.1	−4.2, −8.3	2.16, 2.17	103.8, 99.5	−121.9, −128.6	136.8, 142.0	−99.5, −93.3	809.35
syn-s-*cis*-s-*cis*-*anti*	−14.3, 158.3	1.4, −2.0	−10.290									
				C(α)-*si*	−4.0, 146.7	13.2, 25.4	2.17, 2.17	99.2, 101.9	−125.6, −127.4	140.3, 139.9	−94.7, −95.9	799.02
				C(α)-*re*	−29.9, −38.3	0.4, −165.9	2.17, 2.15	103.9, 106.7	−121.8, −119.4	136.7, 135.7	−99.1, −100.9	825.21
syn-s-*cis*-s-*trans*-*syn*	−15.7, −23.2	17.5, 160.7	−10.505									
				C(α)-*si*	−8.1, −42.1	22.3, −173.5	2.17, 2.16	101.7, 104.4	−123.4, −122.9	137.8, 137.7	−98.8, −98.3	794.05
				C(α)-*re*	−21.3, −25.5	−4.1, −3.4	2.16, 2.17	104.2, 104.1	−121.7, −122.0	136.3, 136.7	−100.0, −99.6	813.88
bis(*syn*-s-*cis*)	−13.7, −13.7	0.5, 0.5	−10.424									
				C(α)-*si*	−17.7, 5.7	21.5, 11.1	2.15, 2.18	103.8, 97.5	−122.1, −128.0	137.1, 141.7	−98.2, −93.5	809.78
				C(α)-*re*	136.5, 138.4	1.5, −8.4	2.16, 2.16	101.7, 99.6	−127.0, −128.5	140.5, 142.0	−95.1, −93.3	815.71
bis(*anti*-s-*cis*)	160.2, 160.2	−0.2, −0.2	−10.328									
				C(α)-*si*	155.0, 141.6	15.5, 28.6	2.19, 2.15	105.8, 101.3	−123.9, −127.7	137.3, 140.4	−98.7, −95.2	769.67

Table 12. *PM3 Values Calculated for the Cycloaddition and Transition States of* **2a** *to 1-Methoxybuta-1,3-diene*

Conformer	S–N–C=O [°]	O=C–C=O [°]	HOMO [eV]	Trans.st.	S–N–C=O [°]	O=C–C=O [°]	δ(C(α)–C) [Å]	δ(O(β)–C) [Å]	O(1)=S–N–C(2) [°]	O(2)=S–N–C(2) [°]	S–N–C(2)–C(3) [°]	S–N–C(2)–H [°]	Imag. freq. [cm^{-1}]
				C(α)-*re endo*	–39.2	–164.2	2.02	2.03	105.5	–121.0	135.5	–100.2	791.81
				C(α)-*re exo*	–46.4	–166.3	2.04	2.02	103.7	–123.8	137.8	–97.4	792.09
syn-s-*trans*	–24.3	171.0	–10.362										
				C(α)-*si endo*	–40.1	–165.7	2.02	2.03	106.8	–120.1	135.0	–100.3	801.19
				C(α)-*si exo*	–28.3	161.4	2.02	2.03	104.9	–121.2	136.6	–98.7	812.37
				C(α)-*re endo*	117.7	–154.7	2.02	2.03	104.7	–121.9	138.5	–97.2	765.84
				C(α)-*re exo*	124.8	–138.3	2.02	2.05	101.4	–124.8	141.3	–93.9	761.37
anti-s-*trans*	158.7	180.0	–10.470										
				C(α)-*si endo*	139.2	–169.7	2.02	2.05	104.7	–122.4	138.3	–97.7	763.54
				C(α)-*si exo*	99.3	151.4	2.02	2.06	97.9	–131.9	143.3	–92.0	755.57
				C(α)-*re endo*	–14.3	32.2	2.04	2.03	103.4	–122.1	137.2	–98.4	778.76
				C(α)-*re exo*	–15.5	34.9	2.06	2.01	103.6	–121.9	137.2	–98.5	790.15
syn-s-*cis*	–13.9	–1.3	–10.510										
				C(α)-*si endo*	–23.9	–10.4	2.04	2.03	104.1	–121.7	136.5	–99.8	781.10
				C(α)-*si exo*	–21.2	–14.1	2.05	2.01	104.3	–121.3	136.2	–100.2	791.06
				C(α)-*re endo*	141.3	40.3	2.04	2.03	101.2	–128.4	140.7	–94.9	781.22
				C(α)-*re exo*	143.8	43.2	2.05	2.02	101.9	–127.8	140.3	–95.5	791.15
anti-s-*cis*	159.3	0.4	–10.544										
				C(α)-*si endo*	131.9	–18.5	2.05	2.00	98.2	–130.7	143.1	–92.1	800.07
				C(α)-*si exo*	133.5	–24.0	2.06	2.00	97.8	–130.9	143.3	–91.8	804.23

Table 13. *PM3 Values Calculated for the Cycloaddition and Transition States of* **2b** *to Cyclopentadiene*

Conformer	S–N–C=O [°]	O=C–N=O [°]	HOMO [eV]	Trans.st.	S–N–C=O [°]	O=C–N=O [°]	δ(N(α)–C) [Å]	δ(O(β)–C) [Å]	O(1)=S–N–C(2) [°]	O(2)=S–N–C(2) [°]	S–N–C(2)–C(3) [°]	S–N–C(2)–H [°]	Imag. freq. [cm^{-1}]
				N(α)-*re endo*	–30.0	145.7	1.71	2.31	105.5	–121.2	136.3	–98.7	429.85
				N(α)-*re exo*	–23.8	116.8	1.83	2.21	104.8	–120.6	136.6	–98.6	619.66
syn-s-*trans*	–25.3	169.4	–10.057										
				N(α)-*si endo*	–34.5	–176.4	1.65	2.31	105.9	–120.8	136.0	–98.9	374.01
				N(α)-*si exo*	–33.4	–170.4	1.82	2.22	104.5	–121.9	137.4	–97.7	615.61
				N(α)-*re endo*	127.7	–160.7	1.73	2.25	103.5	–123.0	139.3	–96.5	494.24
				N(α)-*re exo*	137.5	–175.7	1.88	2.16	104.5	–122.1	138.4	–97.5	667.57
anti-s-*trans*	156.0	–174.5	–10.027										
				N(α)-*si endo*	135.6	–168.7	1.71	2.31	105.8	–121.3	137.5	–98.4	423.64
				N(α)-*si exo*	130.7	–161.0	1.86	2.18	106.1	–121.8	137.6	–98.2	642.89
				N(α)-*re endo*	–10.4	37.1	1.85	2.13	102.1	–123.8	138.3	–96.9	671.49
				N(α)-*re exo*	–54.1	33.9	1.89	2.12	107.5	–119.6	134.1	–101.4	706.90
syn-s-*cis*	–16.4	–2.1	–10.097										
				N(α)-*si endo*	–32.4	–8.5	1.84	2.15	103.3	–123.3	137.6	–98.1	645.45
				N(α)-*si exo*	–25.7	–27.2	1.89	2.12	103.5	–123.0	137.4	98.0	704.66
				N(α)-*re endo*	159.1	41.8	1.85	2.13	104.3	–123.4	137.6	–98.3	666.41
				N(α)-*re exo*	155.3	40.6	1.88	2.13	103.7	–123.6	137.9	–97.9	695.35
anti-s-*cis*	166.6	1.8	–10.031										
				N(α)-*si endo*	142.7	–8.5	1.84	2.14	101.0	–126.5	140.7	–94.8	630.17
				N(α)-*si exo*	154.4	–19.3	1.90	2.11	102.4	–124.4	139.2	–96.5	704.62

Table 14. *STO3-21G Values for the* anti-*s*-cis *and* syn-*s*-cis *Conformers of (−)-***1a, b** *and* **2a, b**

Conformer	S–N–C=O [°]	O=C–X=Y [°]	*ΔhN* [Å]	ΔH_{form} [Hartree]	HOMO [eV]	LUMO [eV]	N-*re* at. coef.	C(O)-*re* at. coef.	X-*re* at. coef.	Y-*re* at. coef.	N-*si* at. coef.	C(O)-*si* at. coef.	X-*si* at. coef.	Y-*si* at. coef.
(−)-**1a** *syn*-s-*cis*	−15.4	−5.9	0.077	−1173.660471	−10.662	2.638	0.063	−0.142	*−0.128*	*0.179*	−0.063	0.134	0.113	−0.180
anti-s-*cis*	158.0	−10.7	0.123	−1173.672378	−10.673	2.807	−0.064	0.136	0.112	−0.183	0.062	−0.143	*−0.113*	*0.186*
(−)-**1b** *syn*-s-*cis*	−15.6	−5.1	0.079	−1212.486435	−10.399	2.842	0.056	−0.145	*−0.109*	*0.206*	−0.066	0.135	0.108	−0.193
anti-s-*cis*	157.7	−10.2	0.123	−1212.498393	−10.214	2.999	−0.056	0.149	0.098	−0.192	0.062	−0.133	*−0.103*	*0.190*
2a *syn*-s-*cis*	−14.8	−16.6	0.047	−1209.269449	−11.128	1.781	−0.071	0.118	0.156	−0.249	0.058	−0.124	*0.169*	*−0.248*
anti-s-*cis*	159.5	−11.6	0.133	−1209.282257	−11.241	1.995	0.076	−0.136	*−0.159*	*0.253*	−0.069	0.151	0.160	−0.243
2b *syn*-s-*cis*	−13.1	−7.0	0.085	−1225.090630	−11.299	0.948	−0.080	0.120	0.275	−0.420	0.070	−0.125	0.255	−0.424
anti-s-*cis*	168.3	−3.4	0.101	−1225.095322	−11.254	1.157	0.095	−0.130	*−0.265*	*0.363*	−0.085	0.135	0.272	−0.335

Table 15. *X-Ray Structure, PM3, AM1, and STO 3-21 G Comparative Geometry for (−)-***1a, b, d, e**, *(−)-***2f** *and (−)-***3b**

		(−)-**1a**				(−)-**1b**				(−)-**1d**			
		X-Ray	PM3	AM1	STO3-21G	X-Ray	PM3	AM1	STO3-21G	X-Ray	PM3	AM1	STO3-21G
S–N–C=O	[°]	153.9	158.5	174.7	158.0	150.8	158.3	174.5	157.7	134.8	144.6	166.2	147.9
O=C–C=C	[°]	1.0	−2.2	−1.9	−10.7	−6.1	−2.3	−2.1	−10.2	140.2	135.6	133.9	142.2
ΔhN	[Å]	0.226	0.152	0.031	0.123	0.230	0.152	0.033	0.123	0.304	0.196	0.068	0.203
		(−)-**1e**				(−)-**2f**				(−)-**3b**			
		X-Ray	PM3	AM1	STO3-21G	X-Ray	PM3	AM1	STO3-21G	X-Ray	PM3	AM1	STO3-21G
S–N–C=O	[°]	140.2	146.1	166.7	146.0	−9.3	−14.6	−3.9	−18.0	148.9	148.3	166.8	168.6
O=C–C=C	[°]	134.0	130.2	131.5	136.8	121.2	119.0	121.3	170.1	−11.9	−3.5	2.3	8.2
ΔhN	[Å]	0.308	0.191	0.064	0.218	0.083	0.105	0.047	0.070	0.200	0.148	0.076	0.09

Table 16. *PM3 Values Calculated for the Cycloaddition and Transition States of (−)-***3a** *to Cyclopentadiene*

Conformer	S–N–C=O [°]	O=C–C=O [°]	HOMO [eV]	Trans.st.	S–N–C=O [°]	O=C–C=O [°]	δ(C(α)–C) [Å]	δ(C(β)–C) [Å]	O(1)=S–N–C(2) [°]	O(2)=S–N–C(2) [°]	S–N–C(2)–C(3) [°]	S–N–C(2)–H [°]	Imag. freq. [cm^{-1}]
				C(α)-*re*	−18.4	−156.5	2.21	2.08	125.0	−100.2	106.4	−133.0	873.33
syn-s-*trans*	−15.8	161.0	−10.170										
				C(α)-*si*	−16.1	−163.6	2.21	2.09	122.4	−102.5	109.0	−130.0	863.55
				C(α)-*re*	95.15	−172.3	2.23	2.07	117.3	−112.3	118.8	−120.1	852.95
anti-s-*trans*	−170.7	−161.1	−10.273										
				C(α)-*si*	117.8	170.2	2.22	2.07	118.7	−110.5	118.0	−120.9	864.73
				C(α)-*re*	−6.7	−1.0	2.22	2.08	118.2	−106.9	113.1	−125.0	860.10
syn-s-*cis*	−14.4	−4.1	−10.182										
				C(α)-*si*	−20.7	27.0	2.23	2.07	124.3	−101.0	105.9	−133.0	856.17
				C(α)-*re*	156.4	−7.0	2.24	2.06	120.9	−108.4	113.6	−124.9	853.10
anti-s-*cis*	169.1	−0.5	−10.199										
				C(α)-*si*	167.0	23.5	2.24	2.06	121.6	−107.6	111.6	−126.7	847.97

Table 17. *PM3 Values Calculated for the Cycloaddition and Transition States of (−)-***3b** *to Cyclopentadiene*

Conformer	S–N–C=O [°]	O=C–C=O [°]	HOMO [eV]	Trans.st.	S–N–C=O [°]	O=C–C=O [°]	δ(C(α)–C) [Å]	δ(C(β)–C) [Å]	O(1)=S–N–C(2) [°]	O(2)=S–N–C(2) [°]	S–N–C(2)–C(3) [°]	S–N–C(2)–H [°]	Imag. freq. [cm^{-1}]
				C(α)-*re*	−43.5	−141.9	2.21	2.09	127.3	−98.8	109.5	−130.3	874.64
syn-s-*trans*	−29.0	162.3	−10.097										
				C(α)-*si*	−37.6	161.5	2.23	2.07	128.6	−97.3	107.4	−132.4	858.44
				C(α)-*re*	95.1	−169.5	2.23	2.07	123.7	−105.8	114.2	−126.5	852.45
anti-s-*trans*	160.2	−155.8	−10.204										
				C(α)-*si*	135.1	157.5	2.20	2.09	123.2	−105.7	115.3	−125.4	217.21
				C(α)-*re*	−25.4	3.1	2.22	2.08	125.2	−99.9	107.8	−131.7	858.56
syn-s-*cis*	−26.1	−2.7	−10.110										
				C(α)-*si*	−56.2	24.2	2.23	2.07	127.7	−98.6	108.4	−131.3	856.06
				C(α)-*re*	151.8	−5.6	2.23	2.07	126.0	−103.3	108.3	−131.2	851.92
anti-s-*cis*	148.3	−3.5	−10.133										
				C(α)-*si*	138.1	33.6	2.24	2.06	125.8	−103.5	110.7	−129.4	846.54

Table 18. *Torsional Angles of Pseudo-Axial and Equatorial Substituents in Dienophiles (−)-***1**, **2** *and* **3** *Based on X-Ray Structure Analyses*

		(−)-**1a**	(−)-**1b**	(−)-**1d**	(−)-**1e**	(−)-**2f**	(−)-**3b**[24])	(+)-**3c** B (A)	(+)-**7c**[39])	(−)-**9**[39])
O(1)=S–N–C(2)	[°]	99.6	103.5	101.9	107.8	102.3	*129.6*	93.6 (90.9)	*137.1*	*136*
O(2)=S–N–C(2)	[°]	−131.1	−125.9	−128.0	−121.5	−126.4	*−99.2*	−137.7 (−140.4)	*−90.2*	*−89*
S–N–C(2)–C(3)	[°]	144.2	142.4	144.3	139.5	141.4	*106.1*	143.3 (148.0)	*101.3*	*98*
S–N–C(2)–H	[°]	−96.3	−98.0	−98.6	−100.6	−92.7	*−135.4*	−97.6 (−94.6)	*−133.8*	*−147*
O(1)···S	[Å]	1.426	1.423	1.421	1.430	1.425	1.434	1.453 (1.452)	1.429	1.44
O(2)···S	[Å]	1.415	1.430	1.412	1.420	1.417	1.429	1.442 (1.438)	1.445	1.43

*(+)-(3aR,6S,7aS)-1,4,6,7,7a-Hexahydro-1-(hydroxyaminocarbonyl)-8,8-dimethyl-3*H*-3a,6-methano[2,1]-benzoisothiazole 3,3-Dioxide* ((+)-(2*S*)-**2e**). Commercially available (+)-(2*S*)-**2c** (100 mg, 0.464 mmol) was added to a suspension of NaH (50% in mineral oil; 26.8 mg, 0.557 mmol) in toluene (5 ml) at r.t. under N_2. After 20 min phosgene (20% soln. in toluene; 0.25 ml, 0.511 mmol) was added, and after 2 h at r.t., this soln. was transferred *via* syringe into a suspension of $NH_2OH \cdot HCl$ (48 mg, 0.697 mmol) and K_2CO_3 (193 mg, 1.393 mmol) in Et_2O (5 ml) saturated with H_2O. After 10 h at r.t., the solvent was evaporated and the residue purified by CC (SiO_2, cyclohexane/AcOEt 2:1): pure (+)-(2*S*)-**2e** (20%) besides (+)-(2*S*)-**2c** (63%). $[\alpha]_D^{20} = +74.9$ ($c = 0.63$, $CHCl_3$). IR (KBr): 3350, 3245, 2961, 1689, 1510, 1323, 1295, 1168, 1135, 994, 882. ^{1}H-NMR: 1.33–1.39 (*m*, 1 H); 1.50 (*t*, $J = 9.3$, 1 H); 1.84–1.93 (*m*, 3 H); 2.02 (*dd*, $J = 13.8$, 8.0, 1 H); 2.12 (*m*, 1 H); 3.39 (*s*, 2 H); 3.87 (*dd*, $J = 7.5$, 4.8, 1 H); 7.90 (br. *s*, 2 H). ^{13}C-NMR: 19.9 (*q*); 20.3 (*q*); 26.6 (*t*); 32.2 (*t*); 37.3 (*t*); 44.3 (*d*); 48.0 (*s*); 49.6 (*s*); 51.8 (*t*); 64.3 (*d*); 152.9 (*s*). CI-MS: 292 (18, $[M + NH_4]^+$), 275 (13), 233 (100, $[\mathbf{2c} + NH_4]^+$), 216 (61), 152 (13).

*(+)-(3aR,6S,7aS)-1,4,5,6,7,7a-Hexahydro-8,8-dimethyl-1-[(1′S,4′R)-2′-oxa-3′-azabicyclo[2.2.1]hept-5′-en-3′-ylcarbonyl]-3*H*-3a,6-methano[2,1]benzoisothiazole 2,2-Dioxide* ((+)-(2*S*,1′*S*,4′*R*)-**5a**). A soln. of (+)-(2*S*)-**2e** (50 mg, 0.182 mmol) in CH_2Cl_2 (1.8 ml) was added dropwise to a suspension of Et_4NIO_4 (65 mg, 0.183 mmol) in cyclopentadiene (60 mg, 0.910 mmol) and CH_2Cl_2 (0.12 ml). After 3 h at r.t., the black soln. was diluted with Et_2O (50 ml), then washed successively with 5% aq. $KHCO_3$ and aq. sat. NaCl soln., dried (Na_2SO_4), filtered, and evaporated. The crude material (94%) was purified by CC (SiO_2, CH_2Cl_2/AcOEt/cyclohexane 2:1:2): pure (+)-(2*S*,1′*S*,4′*R*)-**5a** (50%) besides (+)-(2*S*)-**2c** (13%). M.p. (AcOEt/hexane) 174–175° (dec.). $[\alpha]_D^{20} = +94.6$ ($c = 0.24$, $CHCl_3$). IR: 3020, 2963, 1712, 1331, 1288, 1192, 1144, 931, 846. ^{1}H-NMR: 0.99 (*s*, 3 H); 1.25 (*s*, 3 H); 1.31–1.51 (*m*, 2 H); 1.74 (*d*, $J = 9.1$, 1 H); 1.77 (*ddd*, $J = 13.5$, 7.3, 3.7, 1 H); 1.88–1.96 (*m*, 4 H); 2.13 (*dt*, $J = 8.7$, 2.0, 1 H); 3.44 (s, 2 H); 4.00 (*dd*, $J = 7.8$, 4.4, 1 H); 5.35 (*m*, 1 H); 5.55 (*m*, 1 H); 6.23 (*dt*, $J = 5.6$, 2.0, 1 H); 6.47 (*ddd*, $J = 5.5$, 2.4, 1.6, 1 H). ^{13}C-NMR: 19.9 (*q*); 20.6 (*q*); 26.7 (*t*); 32.5 (*t*); 37.3 (*t*); 44.7 (*d*); 47.9 (*s*); 48.3 (*t*); 48.6 (*s*); 52.7 (*t*); 64.9 (*d*); 69.1 (*d*); 84.6 (*d*); 131.3 (*d*); 133.6 (*d*); 156.1 (*s*). CI-MS: 356 (84, $[M + NH_4]^+$), 339 (91), 292 (25), 276 (10), 250 (10), 233 (100), 217 (7), 152 (7).

*(3aR,6S,7aS)-1,4,5,6,7,7a-Hexahydro-8,8-dimethyl-1-[(1′R,4′S)-2′-oxa-3′-azabicyclo[2.2.1]hept-5′-en-3′-ylcarbonyl]-3*H*-3a,6-methano[2,1]benzoisothiazole 2,2-Dioxide* ((2*S*,1′*R*,4′*S*)-**5a**). Cl_2 (obtained by dropwise addition of conc. HCl soln. (8.62 ml, *ca.* 100 mmol) on $KMnO_4$ (1.34 g, 8.5 mmol)) was bubbled through a glass tube into a soln. of commercial cyclohexanone oxime (2.0 g, 17.67 mmol) in Et_2O (20 ml) [82]. The deep blue soln. was purged with N_2, diluted with Et_2O (30 ml), washed with H_2O, dried (Na_2SO_4), and filtered. The solvent was reduced under vacuum to 24 ml, then EtOH (8 ml) and cyclopentadiene (4.322 g, 65.38 mmol) were added. After decolouration, the white precipitate was filtered and dried under vacuum to give crude *rac*-**4a** (0.636 g, 4.76 mmol), further kept under N_2 in Et_2O soln. due to decomposition [38]. (+)-(2*S*)-**2c** (513 mg, 2.38 mmol) was added to a suspension of NaH (50% in mineral oil; 171 mg, 3.56 mmol) in toluene (5 ml). After 0.5 h at r.t., phosgene (20% soln. in toluene; 2.59 ml, 5.237 mmol) was added, and after an additional 0.5 h, this mixture was transferred *via* syringe to a suspension of K_2CO_3 (658 mg, 4.76 mmol) and the *rac*-**4a** prepared above, in Et_2O (12 ml) saturated with H_2O. After 1 h, the mixture was diluted with Et_2O (50 ml), washed with aq. sat. NaCl, dried (Na_2SO_4), filtered, and evaporated to give crude (2*S*,1′*S*,4′*R*)-**5a**/(2*S*,1′*R*,4′*S*)-**5a**/(2*S*)-**2c** 30:53:17. Purification by CC (SiO_2 [83]) afforded a 40:57.4:2.6 mixture in 50% yield[46]). Data of (2*S*,1′*R*,4′*S*)-**5a** in the mixture. ^{1}H-NMR: 0.97 (*s*, 3 H); 1.20 (*s*, 3 H); 3.45 (*dd*, $J = 13.9$, 13.5, 1 H); 4.05 (*dd*, $J = 7.5$, 4.4, 1 H); 5.21 (br. *s*, 1 H); 5.32 (br. *s*, 1 H); 6.43 (*ddd*, $J = 5.6$, 2.3, 1.7, 1 H); 6.66 (*dt*, $J = 5.6$, 1.9, 1 H). ^{13}C-NMR: 20.0 (*q*); 21.3 (*q*); 26.5 (*t*); 33.1 (*t*); 38.2 (*t*); 45.2 (*d*); 47.7 (*s*); 47.9 (*t*); 48.4 (*s*); 53.1 (*t*); 66.1 (*d*); 67.6 (*d*); 84.0 (*d*); 134.6 (*d*); 137.5 (*d*); 156.0 (*s*).

REFERENCES

[1] J. Jurczak, T. Bauer, C. Chapuis, 'Houben-Weyl, Stereoselective Synthesis', Eds. G. Helmchen, R. W. Hoffmann, J. Mulzer and E. Schaumann, Thieme Verlag, Stuttgart, 1995, Vol. E21c, p. 2735, 2905.

[2] W. Oppolzer, *Tetrahedron* **1987,** *43,* 1969; *Erratum, ibid.* **1987,** *43,* 4057; O. Reiser, *Nachr. Chem. Tech. Lab.* **1996** *44,* 612.

[3] W. Oppolzer, C. Chapuis, G. Bernardinelli, *Helv. Chim. Acta* **1984,** *67,* 1397.

[4] C. Chapuis, Ph. D. Thesis, Université de Genève, 1984, No. 2144, p. 46, 51, 56.

[5] a) W. Oppolzer, G. Poli, C. Starkemann, G. Bernardinelli, *Tetrahedron Lett.* **1988,** *29,* 3559; b) W. Oppolzer, *Pure Appl. Chem.* **1990,** *62,* 1241.

[46]) Enriched material (20:77:3) was obtained in the mother liquors after their repeated recrystallizations.

[6] U. Pindur, G. Lutz, G. Fischer, W. Massa, L. Schröder, D. Schollmeyer, *Tetrahedron* **1993,** *49,* 2863; U. Pindur, G. Lutz, W. Massa, L. Schröder, *Heterocycles* **1993,** *36,* 661.
[7] V. Gouverneur, G. Dive, L. Ghosez, *Tetrahedron: Asymmetry* **1991,** *2,* 1173.
[8] W. Oppolzer, *Angew. Chem. Int. Ed.* **1984,** *23,* 876.
[9] B.H. Kim, D.P. Curran, *Tetrahedron* **1993,** *49,* 293.
[10] D.P. Curran, B.H. Kim, J. Daugherty, T.A. Heffner, *Tetrahedron Lett.* **1988,** *29,* 3555.
[11] K. Iseki, S. Oishi, Y. Kobayashi, *Chem. Lett.* **1994,** 1135.
[12] Y. Makino, K. Iseki, K. Fujii, S. Oishi, T. Hirano, Y. Kobayashi, *Tetrahedron Lett.* **1995,** *36,* 6527.
[13] K. Müller, A. Eschenmoser, *Helv. Chim. Acta* **1969,** *52,* 1823; A. Kümin, E. Maverik, P. Seiler, N. Vanier, L. Damm, R. Hobi, J. Dunitz, A. Eschenmoser, *ibid.* **1980,** *63,* 1158; P. Magnus, T. Gallagher, P. Brown, J.C. Huffman, *J. Am. Chem. Soc.* **1984,** *106,* 2105; A.I. Meyers, B.A. Lefker, K.T. Wanner, R.A. Aitken, *J. Org. Chem.* **1986,** *51,* 1936; D. Seebach, E. Juaristi, D.D. Miller, C. Schrickli, T. Weber, *Helv. Chim. Acta* **1987,** *70,* 237; W. Oppolzer, J.-P. Barras, *ibid.* **1987,** *70,* 1666; W. Oppolzer, G. Poli, *ibid.* **1987,** *70,* 2201.
[14] C. Chapuis, R. Rzepecki, T. Bauer, J. Jurczak, *Helv. Chim. Acta* **1995,** *78,* 145.
[15] W. Oppolzer, B.M. Seletsky, G. Bernardinelli, *Tetrahedron Lett.* **1994,** *35,* 3509.
[16] D.P. Curran, T.A. Heffner, *J. Org. Chem.* **1990,** *55,* 4585.
[17] W.J. Tsai, Y.T. Lin, B.-J. Uang, *Tetrahedron: Asymmetry* **1994,** *5,* 1195.
[18] J.I. Seeman, *Chem. Rev.* **1983,** *83,* 83.
[19] G. Klopman, *J. Am. Chem. Soc.* **1968,** *90,* 223.
[20] L. Salem, *J. Am. Chem. Soc.* **1968,** *90,* 543, 553.
[21] M. Arbelot, A. Allouche, K. Purcell, M. Chanon, *J. Org. Chem.* **1995,** *60,* 2330.
[22] I. Fleming, 'Frontier Orbitals and Organic Chemical Reactions', J. Wiley, New York, 1976.
[23] B. Pascual-Teresa, J. Gonzalez, A. Asensio, K.N. Houk, *J. Am. Chem. Soc.* **1995,** *117,* 4347; K.N. Houk, J. Gonzalez, Y. Li, *Acc. Chem. Res.* **1995,** *28,* 81; L.F. Tietze, G. Schulz, *Liebigs Ann.* **1995,** 1921; B. Stammen, U. Berlage, R. Kindermann, M. Kaiser, B. Günther, W.S. Scheldrick, P. Welzel, W. Roth, *J. Org. Chem.* **1992,** *57,* 6566; D.P. Curran, B.H. Kim, H.P. Piyasena, R.J. Loncharich, K.N. Houk, *ibid.* **1987,** *52,* 2137.
[24] S. Fukuzumi, T. Okamoto, M. Fujita, J. Otera, *J. Chem. Soc., Chem. Commun.* **1996,** 393.
[25] S.E. Denmark, N.G. Almstead, *J. Am. Chem. Soc.* **1993,** *115,* 3133.
[26] D.K. Singh, J.B. Springer, P.A. Goodson, R.C. Corcoran, *J. Org. Chem.* **1996,** *61,* 1436; J.B. Springer, R.C. Corcoran, *ibid.* **1996,** *61,* 1443; R.C. Corcoran, J. Ma, *J. Am. Chem. Soc.* **1991,** *113,* 8973.
[27] W. Oppolzer, I. Rodriguez, J. Blagg, G. Bernardinelli, *Helv. Chim. Acta* **1989,** *72,* 123.
[28] K.S. Kim, B.H. Kim, W.M. Park, S.J. Cho, B.J. Mhin, *J. Am. Chem. Soc.* **1993,** *115,* 7472.
[29] W. Oppolzer, presented at the 'First Anglo-Normand Organic Chemistry Colloqium', Rouen, France, May 1991.
[30] L.M. Tolber, M.B. Ali, *J. Am. Chem. Soc.* **1985,** *107,* 4589; *ibid.* **1984,** *106,* 3806; *ibid.* **1982,** *104,* 1742; *ibid.* **1981,** *103,* 2104.
[31] T. Bauer, C. Chapuis, J. Kozak, J. Jurczak, *Helv. Chim. Acta* **1989,** *72,* 482.
[32] T. Bauer, C. Chapuis, A. Jezewski, J. Kozak, J. Jurczak, *Tetrahedron: Asymmetry* **1996,** *7,* 1391.
[33] J. Jurczak, *Pol. J. Chem.* **1979,** *53,* 2539; J. Jurczak, M. Tkacz, *J. Org. Chem.* **1979,** *44,* 3347.
[34] a) T. Bauer, C. Chapuis, J. Kiegel, J.W. Krajewski, K. Piechota, Z. Urbanczyk-Lipkowska, J. Jurczak, *Helv. Chim. Acta* **1996,** *79,* 1059; b) R.S. Ward, A. Pelter, D. Goubet, M.C. Pritchard, *Tetrahedron: Asymmetry* **1995,** *6,* 93; c) *ibid.* **1995,** *6,* 469.
[35] a) W. Oppolzer, M. Wills, M.J. Kelly, M. Signer, J. Blagg, *Tetrahedron Lett.* **1990,** *31,* 5015; b) W. Oppolzer, A.J. Kingma, S.K. Pillai, *ibid.* **1991,** *32,* 4893.
[36] a) G. Bernardinelli (Department of Organic Chemistry, University of Geneva, CH–1211 Geneva 4), private communication; b) V. Martinez-Merino, I. Garcia, J.A. Mayoral, M.J. Gil, J.M. Zabalza, J.P. Fayet, M.C. Vertut, A. Carpy, A. Gonzalez, *Tetrahedron* **1996,** *52,* 8947.
[37] G.M. Steinberg, J. Bolger, *J. Org. Chem.* **1956,** *21,* 660; R.E. Oesper, W. Broker, *J. Am. Chem. Soc.* **1925,** *47,* 2606; A. Defoin, A. Brouillard-Poichet, J. Streith, *Helv. Chim. Acta* **1991,** *74,* 103; J.B. Behr, A. Defoin, N. Mahmood, J. Streith, *Helv. Chim. Acta* **1995,** *78,* 1166.
[38] a) D. Ranganathan, S. Ranganathan, C.B. Rao, K. Raman, *Tetrahedron* **1981,** *37,* 629; b) S.F. Martin, M. Hartmann, J.A. Josey, *Tetrahedron Lett.* **1992,** *33,* 3583.
[39] P. Deslongchamps, 'Stereoelectronic Effects in Organic Chemistry', Ed. J.E. Baldwin, Pergamon Press, Oxford, 1983; A.J. Kirby, 'The Anomeric Effect and Related Stereoelectronic Effects at Oxygen', Vol. 15 of 'Reactivity and Structure Concepts in Organic Chemistry', Springer Verlag, Berlin, 1983.

[40] W. Oppolzer, M. Wills, C. Starkemann, G. Bernadinelli, *Tetrahedron Lett.* **1990,** *29,* 4117.
[41] J.M. Coxon, K.N. Houk, R.T. Luibrand, *J. Org. Chem.* **1995,** *60,* 418.
[42] A.S. Cieplak, B.D. Tait, C.R. Johnson, *J. Am. Chem. Soc.* **1989,** *111,* 8447.
[43] R.L. Halterman, B.A. Mc Carthy, M.A. Mc Evoy, *J. Org. Chem.* **1992,** *57,* 5585; S. Mataka, J. Ma, T. Thiemann, J.M. Rudzinski, T. Sawada, M. Tashiro, *Tetrahedron Lett.* **1995,** *36,* 6105.
[44] R.A. Poirier, C.C. Pye, J.D. Xidos, D.J. Burnell, *J. Org. Chem.* **1995,** *60,* 2328; L.C. Burry, J.N. Bridson, D.J. Burnell, *ibid.* **1995,** *60,* 5931; N.H. Werstiuk, J. Ma, *Can. J. Chem.* **1994,** *72,* 2493.
[45] G. Mehta, S. Padma, S.H. Krishna Reddy, N. Nethadji, *J. Chem. Soc., Perkin Trans. 1* **1994,** 2049.
[46] G. Mehta, F.A. Khan, W. Adcock, *J. Chem. Soc., Perkin Trans. 2* **1995,** 2189; Y.D. Wu, Y. Li, J. Na, K.N. Houk, *J. Org. Chem.* **1993,** *58,* 4625; S.D. Kahn, W.J. Hehre, *J. Am. Chem. Soc.* **1987,** *109,* 663; S.D. Kahn, C.F. Pau, L.E. Overman, W.J. Hehre, *ibid.* **1986,** *108,* 7381.
[47] A.P. Marchand, U.R. Zope, A. Burritt, S.G. Bott, *Tetrahedron* **1995,** *51,* 9319; P.P.M.A. Dols, A.J.H. Klunder, B. Zwanenburg, *ibid.* **1994,** *50,* 8515.
[48] a) W. Oppolzer, C. Chapuis, G. Bernardinelli, *Tetrahedron Lett.* **1984,** *25,* 5885; b) N. Shida, C. Kabuto, T. Niwa, T. Ebata, Y. Yamamoto, *J. Org. Chem.* **1994,** *59,* 4068; c) G. Riehs, E. Urban, H. Völlenkle, *Tetrahedron* **1996,** *52,* 8725; d) J.F.P. Andrews, A.C. Regan, J.D. Wallis, D.C. Povey, *Acta Crystallogr., Sect. C: Sect. Cryst. Struct. Commun.* **1992,** *48,* 2196.
[49] J.F. King, K.C. Khemeni, S. Skonieczny, N.C. Payne, *J. Chem. Soc., Chem. Commun.* **1988,** 415.
[50] N. Harada, T. Soutome, S. Murai, H. Uda, *Tetrahedron: Asymmetry* **1993,** *4,* 1755.
[51] M. Charton, in 'The Chemistry of Alkenes', Ed. J. Zabicky, Interscience, New York, 1970, Vol. 2, p. 511.
[52] W. Oppolzer, G. Poli, A. Kingma, C. Starkemann, G. Bernardinelli, *Helv. Chim. Acta* **1987,** *73,* 2201.
[53] A. Eschenmoser, M. Dobler, *Helv. Chim. Acta* **1992,** *75,* 218.
[54] C. Chapuis, R. Brauchli, *Helv. Chim. Acta* **1992,** *75,* 1527.
[55] F. Mohamadi, N.G.J. Richards, W.G. Guida, R. Liskamp, M. Lipton, C. Caufield, G. Chang, T. Hendrickson, W.C. Still, *J. Comput. Chem.* **1990,** *11,* 440.
[56] J.L. Marco, N. Martin, A. Martinez-Grau, C. Seoave, A. Albert, F.H. Cano, *Tetrahedron* **1994,** *50,* 3509.
[57] G. Bernardinelli, W. Oppolzer, D. Dupuis, *Acta Crystallogr., Sect. C: Cryst. Struct. Commun.* **1986,** *42,* 1460.
[58] J. Vallgarda, U. Appelberg, I. Csoregh, U. Hacksell, *J. Chem. Soc., Perkin Trans. 1* **1994,** 401.
[59] P.A. Zerotic, X. Weng, C.K. Biggers, M.S. Biggers, M.L. Caspar, D.G. Davis, *Tetrahedron Lett.* **1992,** *33,* 2637.
[60] H. Hagiwara, T. Okamoto, N. Harada, H. Uda, *Tetrahedron* **1995,** *51,* 9891.
[61] D.P. Curran, W. Shen, J. Zhang, T.A. Heffner, *J. Am. Chem. Soc.* **1990,** *112,* 6738.
[62] G. Bernadinelli, W. Oppolzer, P. Schneider, *Acta Crystallogr., Sect. C: Cryst. Struct. Commun.* **1987,** *43,* 1000.
[63] W. Oppolzer, J. De Brabander, E. Walther, G. Bernardinelli, *Tetrahedron Lett.* **1995,** *36,* 4413.
[64] M.J. Wu, C.C. Wu, T.C. Tseng, L.N. Pridgen, *J. Org. Chem.* **1994,** *59,* 7188.
[65] B. Klotz-Berendes, H.J. Schäfer, M. Grehl, R. Fröhlich, *Angew. Chem. Int. Ed.* **1995,** *34,* 189.
[66] W.X. Wu, A.T. Mc Phail, N.A. Porter, *J. Org. Chem.* **1994,** *59,* 1302.
[67] P.A. Garner, W. Bin Ho, S.K. Grandhee, W.J. Youngs, V.O. Kennedy, *J. Org. Chem.* **1991,** *56,* 5893.
[68] T. Bauer, A. Jezewski, C. Chapuis, J. Jurczak, *Tetrahedron: Asymmetry* **1996,** *5,* 1385.
[69] D.P. Curran, S.J. Geib, C.H. Lin, *Tetrahedron: Asymmetry* **1994,** *5,* 199.
[70] J.T. Capron, B.D. Santarsiero, J.C. Vederas, *J. Chem Soc., Chem. Commun.* **1993,** 1074.
[71] B.H. Kim, J.Y. Lee, K. Kim, D. Whang, *Tetrahedron: Asymmetry* **1991,** *2,* 27.
[72] W. Oppolzer, D. Dupuis, G. Poli, T.M. Raynham, G. Bernardinelli, *Tetrahedron Lett.* **1988,** *29,* 5885.
[73] T. Bauer, K. Piechota. K. Kiegiel, J. Jurczak, unpublished results.
[74] N. Harada, T. Soutone, T. Nehira, H. Uda, S. Oi, A. Okamura, S. Miyano, *J. Am. Chem. Soc.* **1993,** *115,* 7547.
[75] R. Freund, C. Allagiannis, P. Schonholzer, K. Bernauer, *Helv. Chim. Acta* **1994,** *77,* 615.
[76] B.H. Kim, Y.J. Chung, G. Keum, J. Kim, K. Kim, *Tetrahedron Lett.* **1992,** *33,* 6811.
[77] S.C. Mayer, A.J. Pfizenmayer, R. Cordova, W.R. Li, M.M. Joullié, *Tetrahedron: Asymmetry* **1994,** *5,* 519.
[78] H. Josien, A. Martin, G. Chassaing, *Tetrahedron Lett.* **1991,** *32,* 6547.
[79] H. Josien, G. Chassaing, *Tetrahedron: Asymmetry* **1992,** *3,* 1351.
[80] N. Harada, T. Hattori, T. Suzuki, A. Okamura, H. Ono, S. Miyano, H. Uda, *Tetrahedron: Asymmetry* **1993,** *4,* 1789.
[81] J.J.P. Stewart, *J. Comput.-Aided Mol. Design* **1990,** *4,* 1.
[82] O. Piloty, H. Steinbock, *Chem. Ber.* **1902,** 3101.
[83] W.C. Still, M. Kahn, A. Mitra, *J. Org. Chem.* **1978,** *43,* 2923.